The Larder Lake Gold Transect; Comparison of the results from various seismic prospecting methods

Mostafa Naghizadeh

PDAC 2023
TORONTO
Saturday, March 4, 2023

METAL EARTH

A new Canadian research initiative funded by Canada First Research Excellence Fund.

CANADA FIRST RESEARCH EXCELLENCE FUND

Canada

LaurentianUniversity
UniversitéLaurentienne
HARQUAIL SCHOOL OF EARTH SCIENCES
ÉCOLE DES SCIENCES DE LA TERRE

MERC
Mineral Exploration Research Centre

Outline

- Introduction
- Active Seismic Applications
  - Conventional Seismic Processing
  - Cross-Dip Move-Out (CDMO) corrections
  - Multi-focusing Imaging
  - Full Wave-Form (FWI) imaging
- Passive Seismic Application
  - Ambient Noise Surface Wave Tomography
  - Receiver Function analysis
- Integration and Interpretations
- Conclusions

METAL EARTH

Introduction

- **Metal Earth** is an applied research and development program led by Laurentian University with $104 million funding from the Canada First Research Excellence Fund and federal/provincial/industry partners.
- By focusing on the **Precambrian Era**, Metal Earth aims to answer fundamental questions related to **differential metal endowment** in both space and time.
- The project intends to determine the **geological, geochemical, and geophysical differences** between metal endowed, less endowed, and barren areas with seemingly equivalent geological settings.
- Metal Earth geophysical data includes **reflection seismic, MagnetoTelluric (MT), gravity, and passive seismic** surveys along several transects in the Archean Superior geological province of Canada, with an overall length of more than 1000 km extending from southeastern Quebec to north-western Ontario.

METAL EARTH

Abitibi and Wabigoon Subprovince of Superior

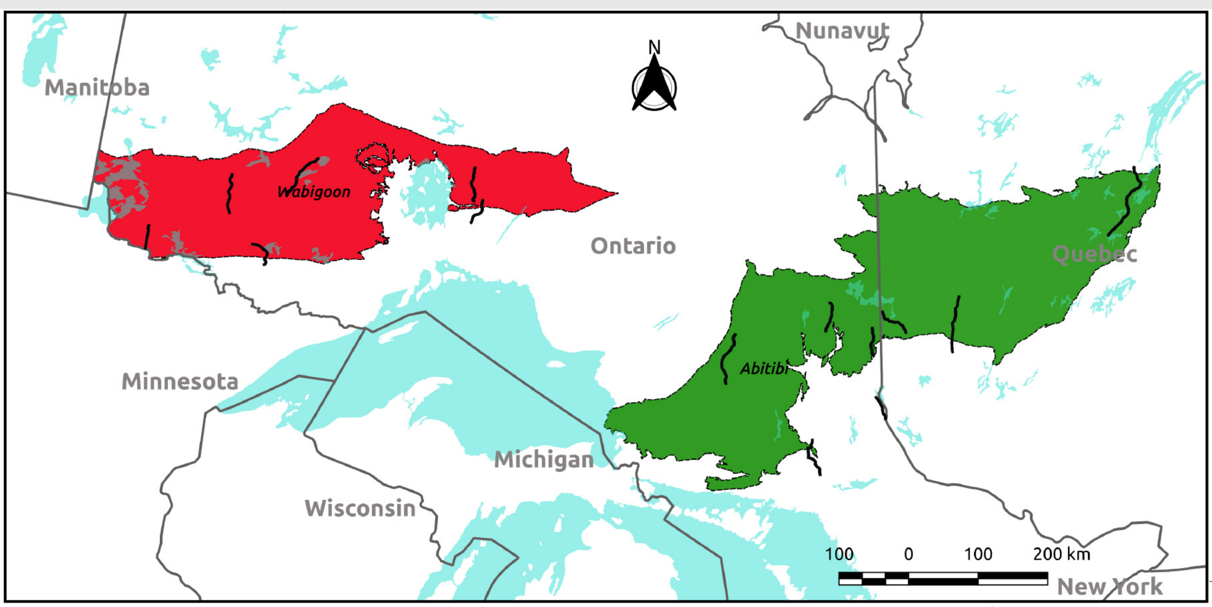

Lithological Map of Superior Province and Seismic Transects

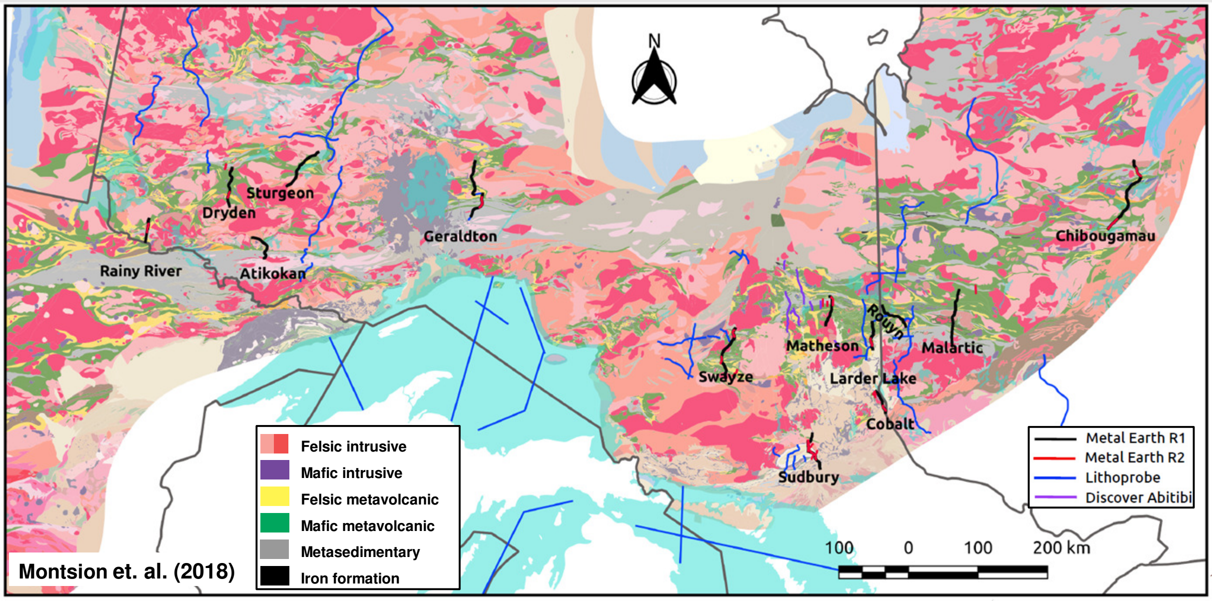

Lithology and Assemblage Map of Larder Lake Area

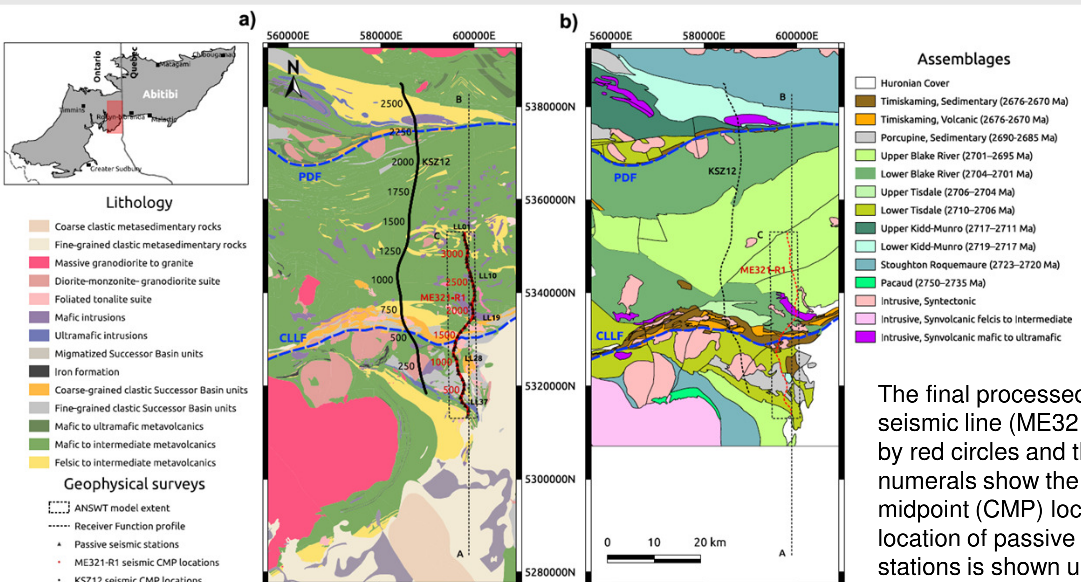

The final processed Larder Lake seismic line (ME321-R1) is shown by red circles and the red color numerals show the common midpoint (CMP) locations. The location of passive seismic stations is shown using filled black triangles that closely follow the ME321 seismic line.

(a) The magnetic anomaly and (b) Bouguer gravity anomaly maps of the Larder Lake area. The reflection seismic transects were shown by thin dashed white lines. The locations of major geological faults (Cadillac-Larder Lake Fault (CLLF) and Porcupine-Destor Fault (PDF)) were shown by thick dashed white lines.

7

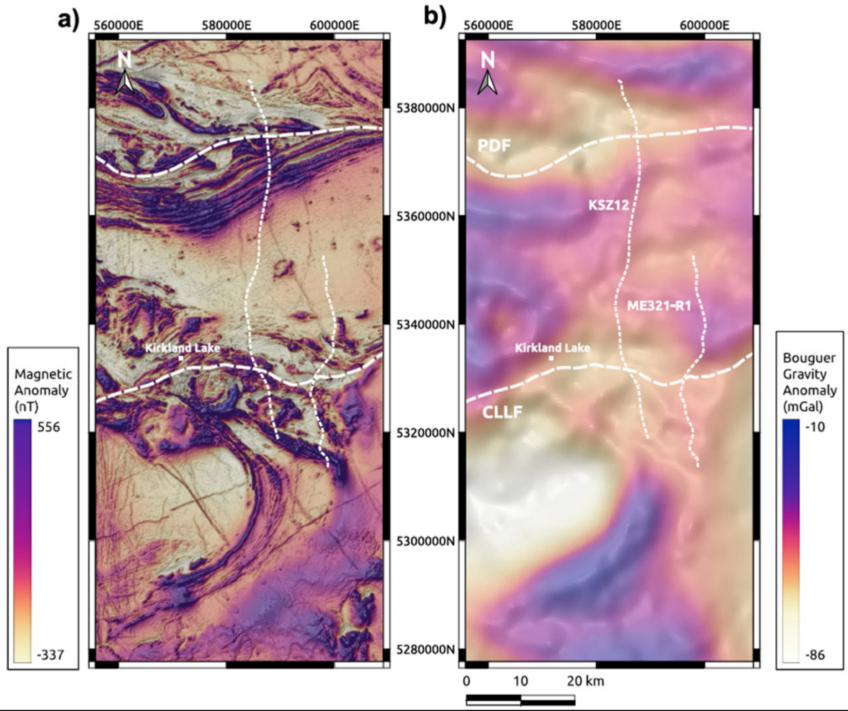

- Introduction
- Active Seismic Applications
  - Conventional Seismic Processing
  - Cross-Dip Move-Out (CDMO) corrections
  - Multi-focusing Imaging
  - Full Wave-Form (FWI) imaging
- Passive Seismic Application
  - Ambient Noise Surface Wave Tomography
  - Receiver Function analysis
- Integration and Interpretations
- Conclusions

METAL EARTH

2D Reflection Seismic Data Acquisition

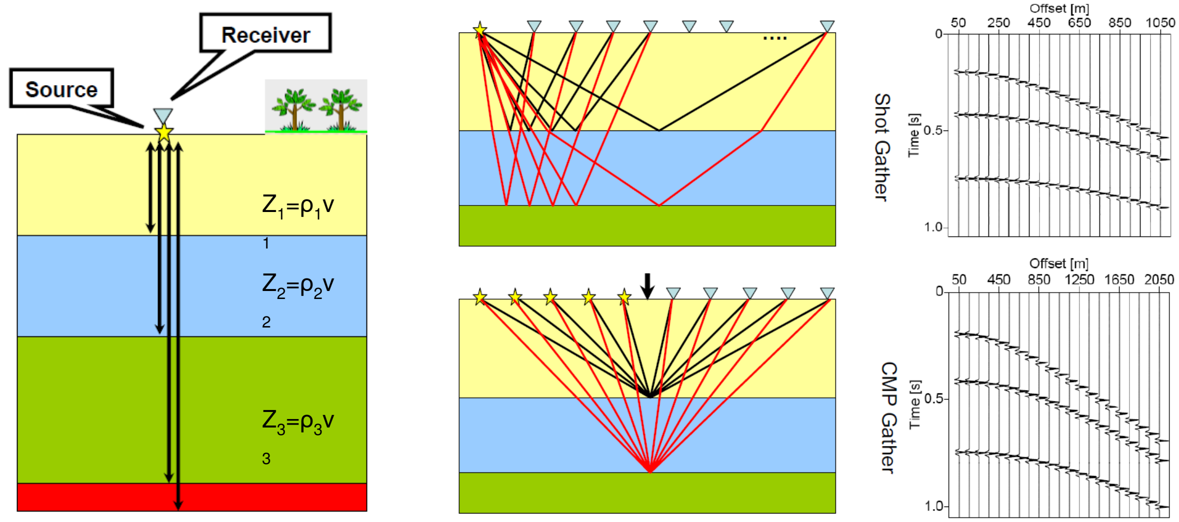

Ideal Reflection Seismic Survey **Practical Reflection Seismic Survey**

METAL EARTH

Metal Earth Seismic Transects -- Acquisition

Metal Earth Seismic Acquisition Parameters

Parameter	Regional (R1) mode	High-Resolution (R2) mode
Record length	12 or 16 s	12 s
Sample rate	2 ms	2 ms
Spread size	15 km-0-15 km	All live (10-20 km)
Roll on/off	Yes	Yes
Source interval	50 m (4 sweeps); 12.5 m (1 sweep)	25 m (4 sweeps); 6.25 m (1 sweep)
Receiver interval	25 m	12.5 m
Vibrator sweep	28 s, 2-96 Hz linear; 4 vibs;	28 s, 5-120 Hz +3db/octave; 3 vibs;

Metal Earth Seismic Transects

Transect Name	Length, km	Acquisition Modes	Comment
Chibougamau	129.85	R1, R2 × 2	No vibrator move-up
Malartic	84.775	R1, R3	Major gap near Malartic Mine/Town
Rouyn-Noranda	84.775	R1, R3	Crooked line; coincident with Lithoprobe AG-21
Larder Lake	49	R1, R2, R3	coincident with Lithoprobe AG-23
Cobalt	46.375	R1, R2	
Matheson	53.95	R1, R2	R1, R2 offset
Swayze	89.35, 11.8	R1, R2 × 3	
Geraldton	60.2125	R1 × 2, R2	Coincident with Lithoprobe WS-3a
Sturgeon Lake	73.475	R1	
Atikokan	54.1	R1	Crooked line
Dryden	74.4	R1, R2 × 2	
Rainy River	33.15	R1, R2	
Sudbury	39, 17, 16, 10	R1 × 3, R2 × 2, R3	Grid of lines

Naghizadeh et. al. (2019)

METAL EARTH

A Seismic Shot Gather from Malartic Transect

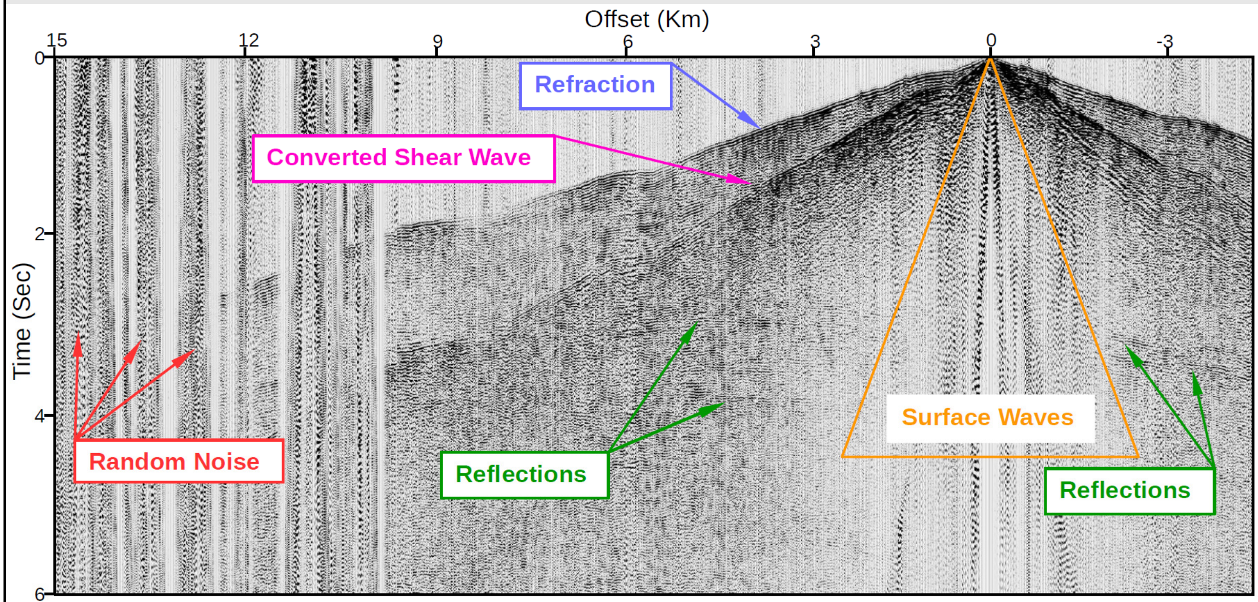

METAL EARTH

Two Important Steps of Seismic Data Processing

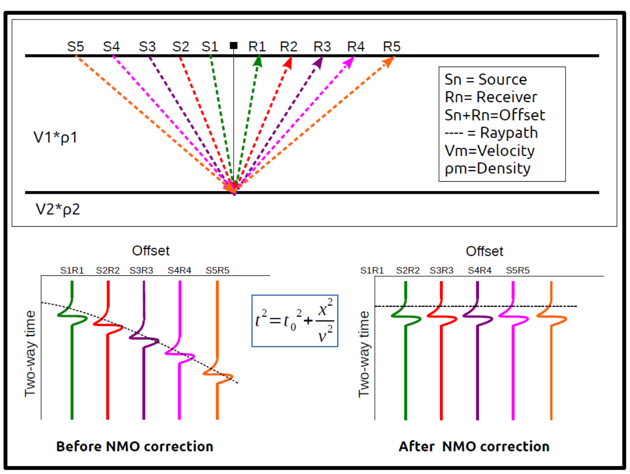

Normal Move-Out (NMO) correction

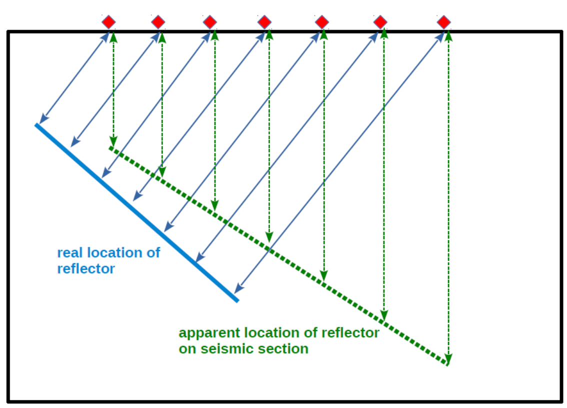

Seismic Migration

METAL EARTH

Metal Earth Seismic Data Processing

Processing Step	Parameters Used	Comment
Trace Kills and Reversals		
Min Phase Conversion		
Ensemble Balance, Amplitude Recovery	Time power correction + 1.5	
Surface Conistent Scaling		
Linear and Erratic Noise Attenuation		
Surface-Consistent Deconvolution	Operator: 160 ms Prewhitening: 0.1 %	Design window: 171-10000 ms at 38 m offset 3347-10000 ms at 15000 m offset
Anomalous Frequency Suppression	Outband: 5-100 Hz Signal band: 15-50 Hz	
Refraction Statics	Datum:500 m Replacement Velocity: 5600 m/s	Tomography
Linear and Erratic Noise Attenuation		
TE Mean window		Design window: 171-10000ms at 38 m offset 3347-10000 ms at 15000 m offset
Velocity Analysis		Every 1.0 km
Surface Consistent Residual Statics	Max shift 64 ms Window: 2000-9000 ms	
Velocity Analysis2		Every 500 m
Surface Consistent Residual Statics	Max shift 48 ms Window: 1000-9000 ms	

METAL EARTH

Metal Earth Seismic Data Processing (cont.)

Post-Stack Time migration		
Velocity Analysis		
Normal Move-out & Mute		
CDP stack		
Time Migration	Kirchhoff Summation	Migration Angle: 65 degrees Max Aperture: 15000 meters
Pre-Stack Time migration (PSTM)		
Velocity Analysis (PSTM)	Kirchhoff Summation	CMP/CDP Distance: $\leq$ 500 meters
Trace Equalization window	Rolling Window: 1000 ms Overlap 50%	
Pre Stack Time Migration (PSTM)	Kirchhoff Summation	Migration Angle: 65 degrees Max Aperture: 10000 meters
Front-End Muting	3/93 1067/758 3554/1871 8028/2778 (m/ms)	
CDP Stack		
Random Noise Attenuation		
TraceEqualization window	Rolling Window: 1000 ms Overlap 50%	

METAL EARTH

CMP to CMP-Line distance (Crooked Line) -- Swayze Transect

Full-Offset (~70 km)

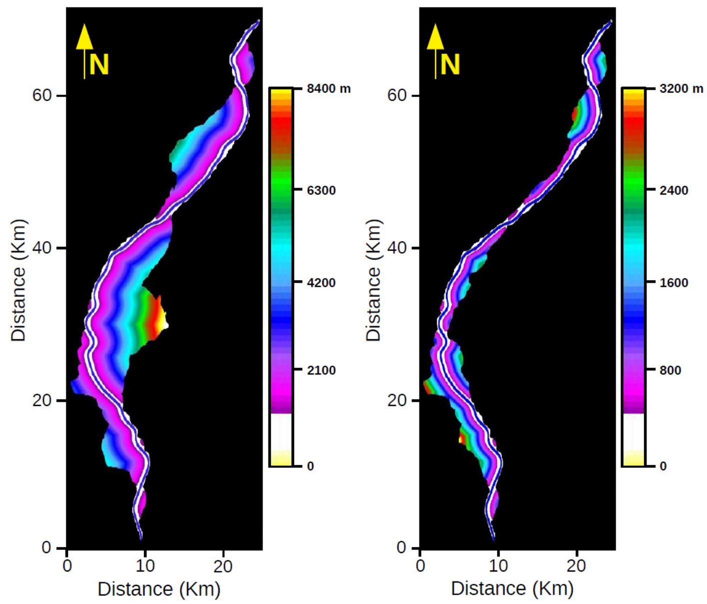

Offset < 15 km

METAL EARTH

Statics Correction for Land Seismic Data

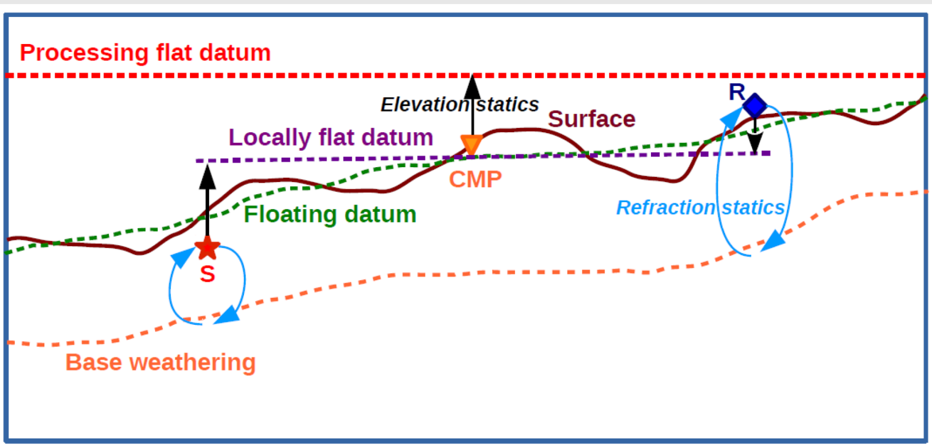

Elevation Statics: To remove the effect of topography
Refraction Statics: To remove the effect of near-surface velocity vatriations
Residual Statics: To remove any random jittered time-shifts in seismic events after correcting the elevation and refraction statics.

METAL EARTH

The Metal Earth Larder Lake ME321-R1 seismic transect processed using conventional seismic data processing flow.

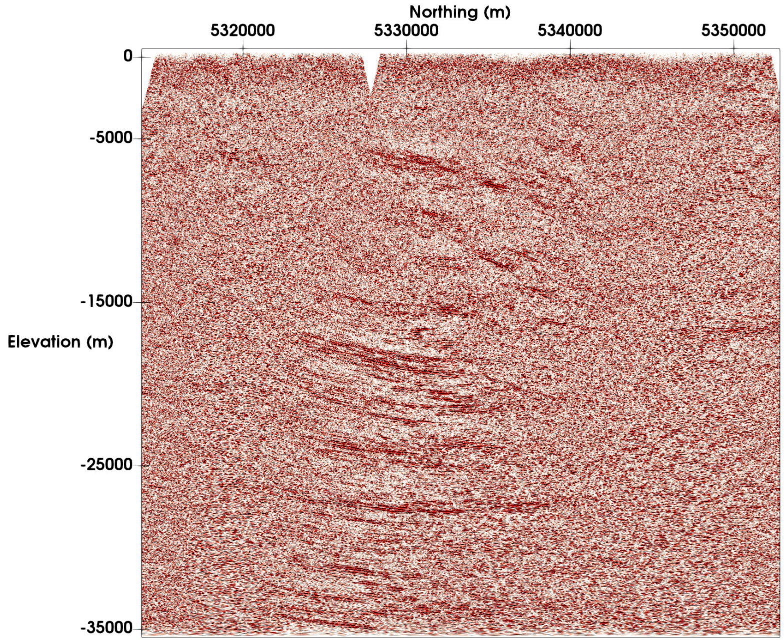

The Metal Earth Larder Lake ME321-R1 seismic transect after applying dip-coherency enhancement.

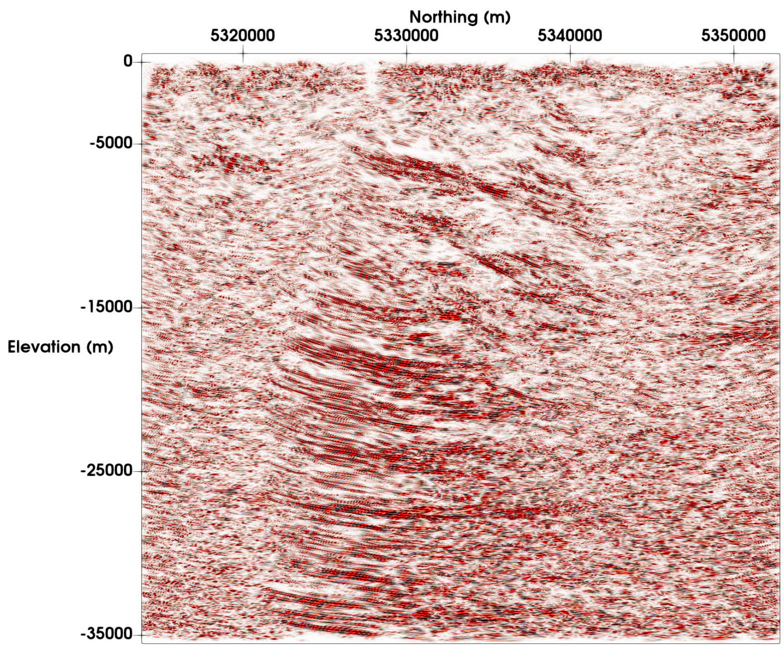

Overlay of electrical resistivity section inverted from Metal Earth's MT data on the Metal Earth Larder Lake ME321-R1 seismic transect after applying dip-coherency enhancement.

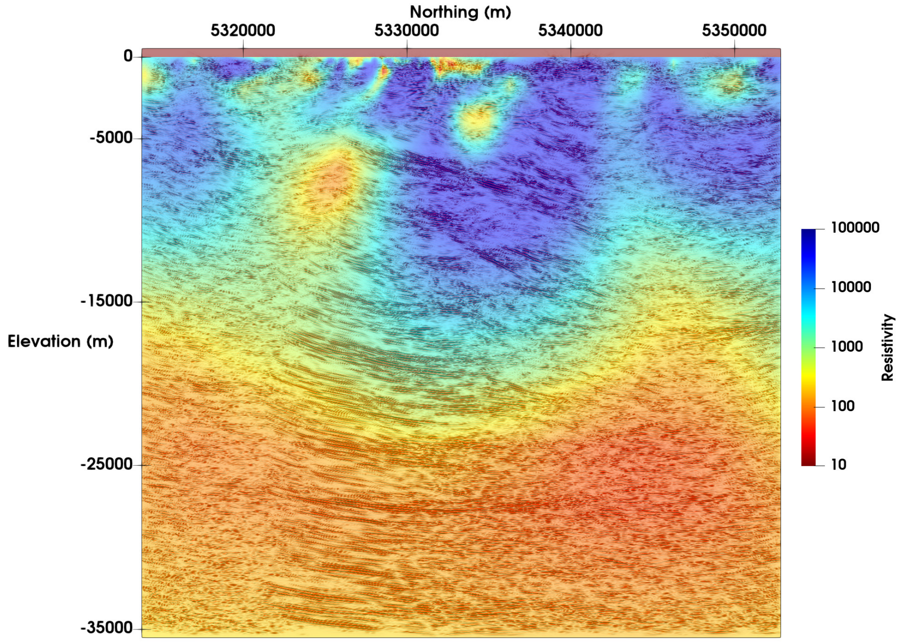

Prospective view of the Metal Earth Larder Lake ME321-R1 seismic transect after applying dip-coherency enhancement with lithology map to the west of the transect.

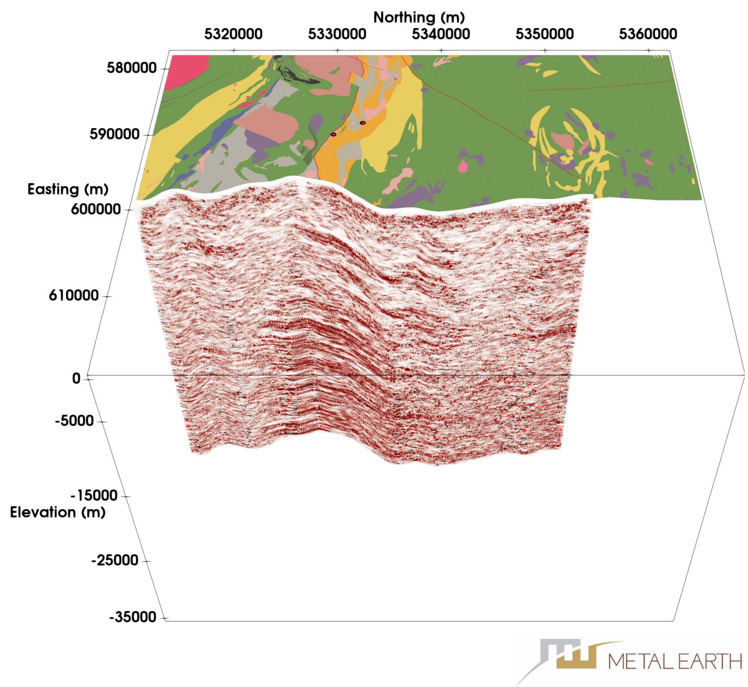

Prospective view of the Metal Earth Larder Lake ME321-R1 seismic transect after applying dip-coherency enhancement and projects electrical resistivity with lithology map to the west of the transect.

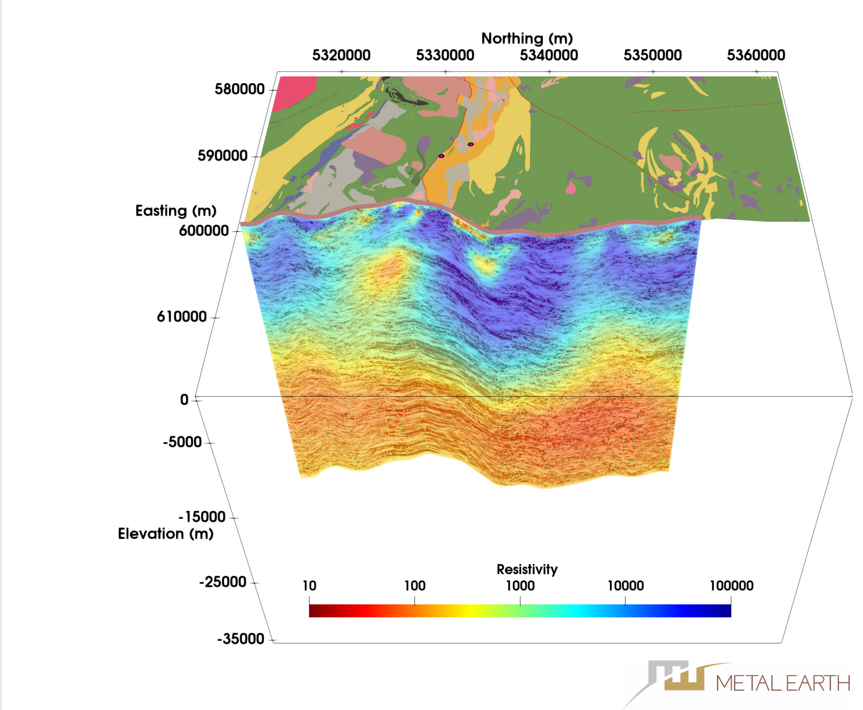

(a) The Metal Earth ME321-R1 seismic transect. (b) The Lithoprobe KSZ12 seismic transect. (c) and (d) are the dip-coherency enhancements of (a) and (b) using the curvelet transform. The plots (a) and (b) are depicted with distance and depth axes, while (c) and (d) are plotted with trace number and time axes. Time to depth conversion of seismic sections was done based on the assumption of constant velocity of 6 km/s. The locations of major geological faults (Cadillac-Larder Lake Fault (CLLF), Porcupine-Destor Fault (PDF), and Lincoln-Nipissing Fault (LNF)) are marked in (c) and (d).

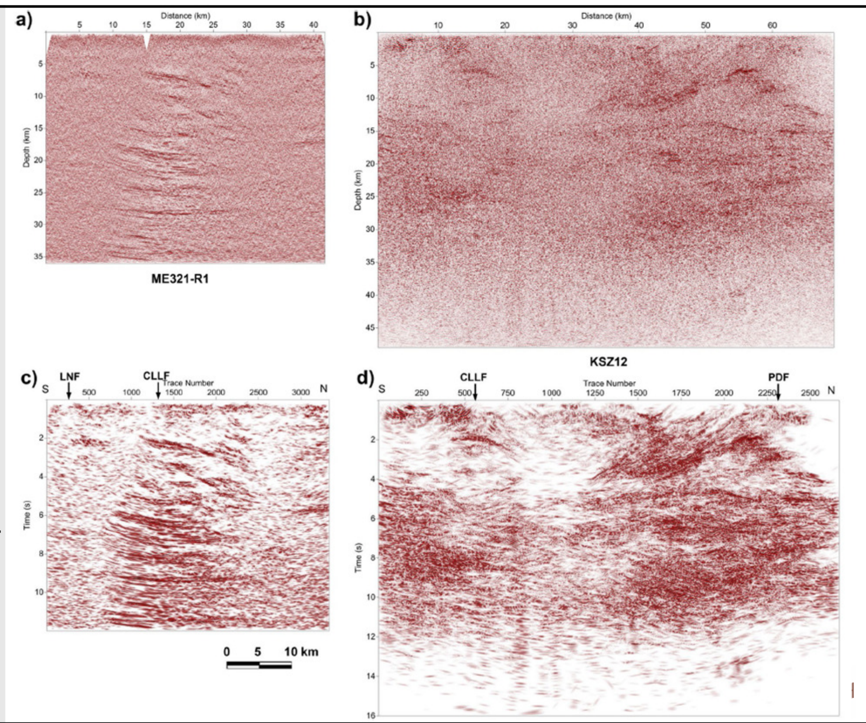

Interpretation of Archean Reflections (Ensimatic – Oceanic setting)

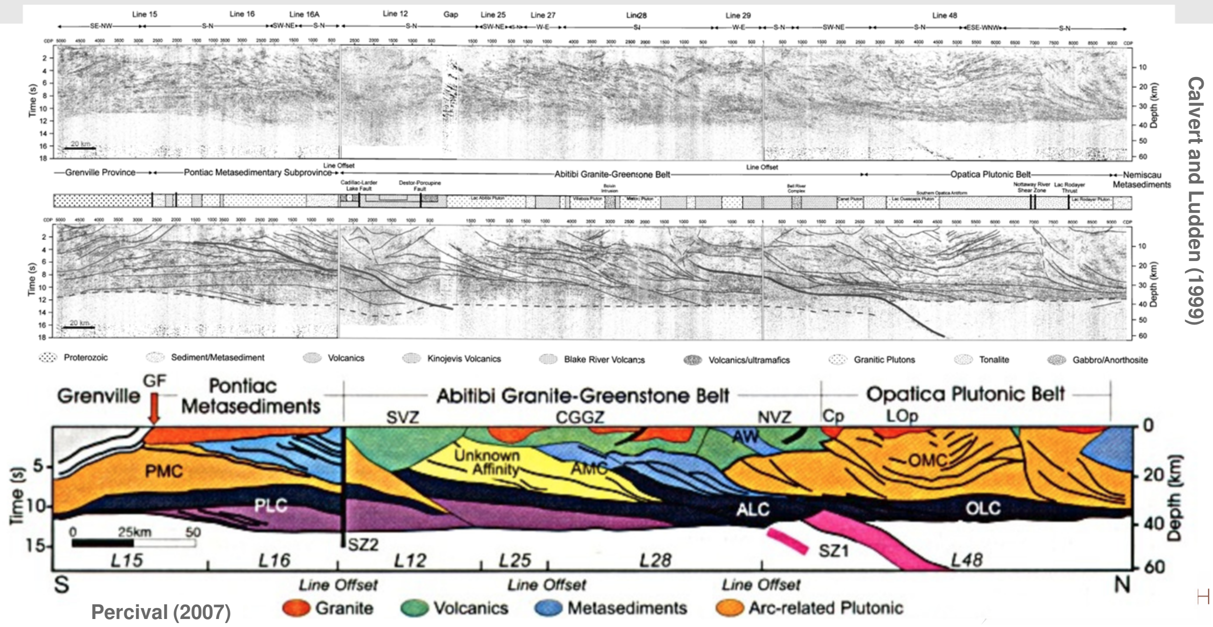

Interpretation of Archean Reflections (Ensialic - Continental setting)

- **Upper Crust** (top 5 to 10 km) is mostly **non-reflective** except across meta-sedimentary belts.
-
- **Middle Crust** reflections are often gently dipping layers with variable thickness of 10 to 20 km. The boundaries of these layers should have a **tectonic origin** as there are variations of slope and cross-cutting of the layers.

- **Lower Crust** layers show zones of **intense and parallel reflections** near the base of the crust. The thickness of this zone in Abitibi is around 10 km while in Wabigoon (western Superior) it doubles to 20 km.

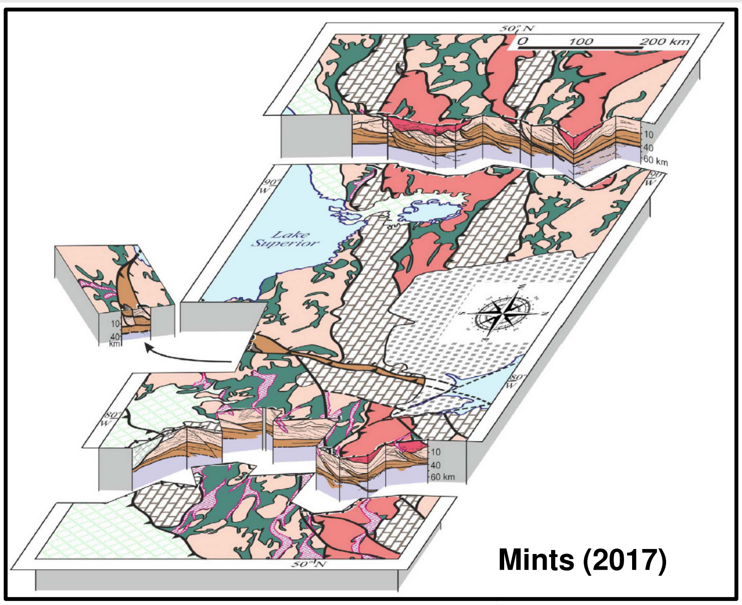

What is the nature of reflections in Archean Superior?

- Lithological Boundaries
- Deformation Zones
- Extensive Mafic Sills
- Trapped Fluids
- Magmatic Underplating
- …

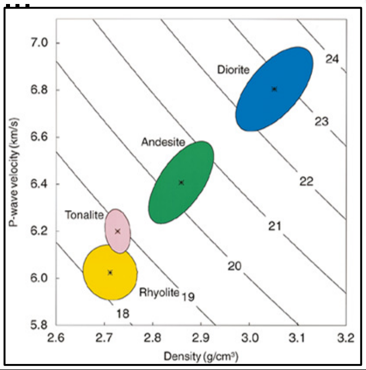

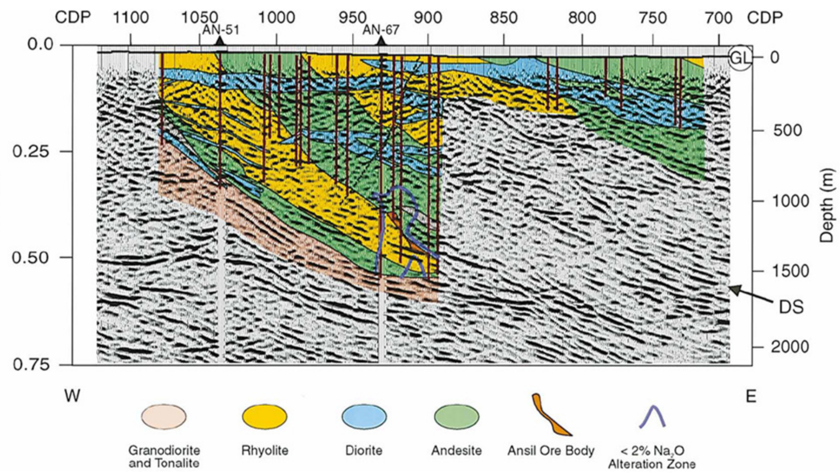

High-resolution Seismic Imaging of Ansil (VMS) mining camp

Perron and Calvert (1998)
van der Velden (2007)

METAL EARTH

- Introduction
- Active Seismic Applications
  - Conventional Seismic Processing
  - Cross-Dip Move-Out (CDMO) corrections
  - Multi-focusing Imaging
  - Full Wave-Form (FWI) imaging
- Passive Seismic Application
  - Ambient Noise Surface Wave Tomography
  - Receiver Function analysis
- Integration and Interpretations
- Conclusions

METAL EARTH

Swath 3D Data

Simple example of a crooked **2D** acquisition line. **3D** "Swath".

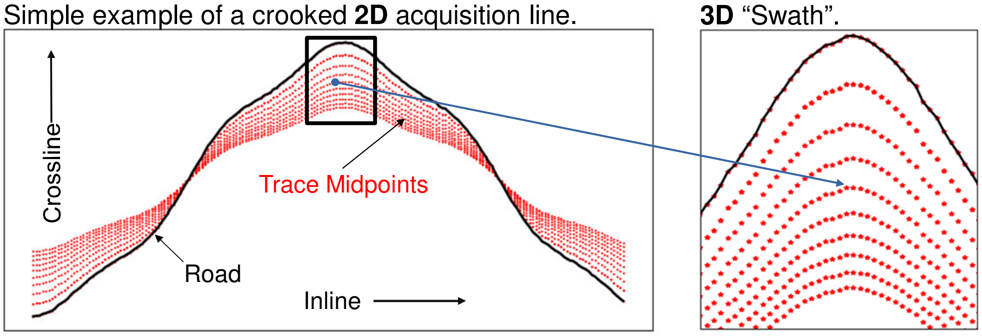

Mid-Points Uneven in Cross-line Direction

METAL EARTH

Binning of a crooked 2D seismic line

Straight Crooked Line Binning

- Simpler

Curved Crooked Line Binning

- Midpoints closer to CMP line

Two CMP line configurations.

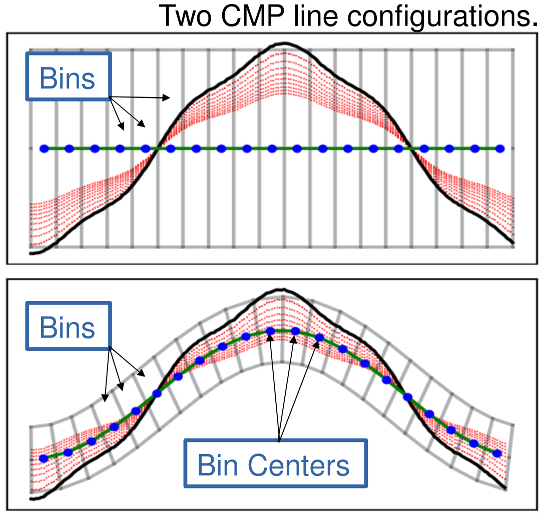

METAL EARTH

Cross Dip Analysis (Example)

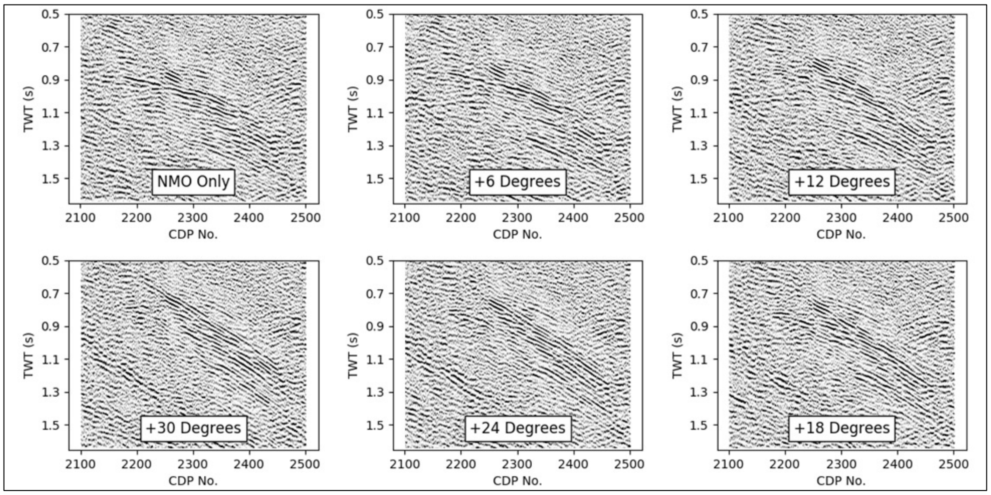

Example of Cross Dip analysis windows applied every 3 degrees in the UTM x direction.

Synthetic Data Comparison (Straight)

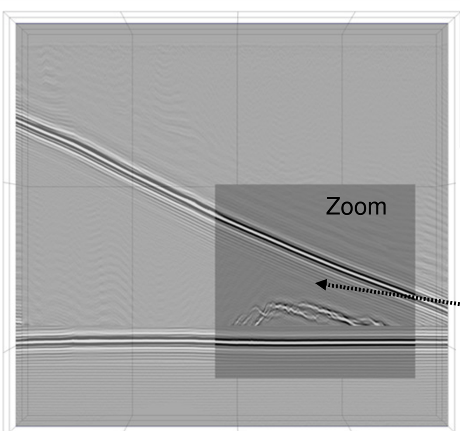

Perspective view of Structure Stack
Straight CMP Line
CDMO Corrected

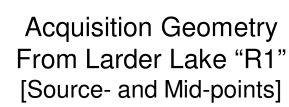

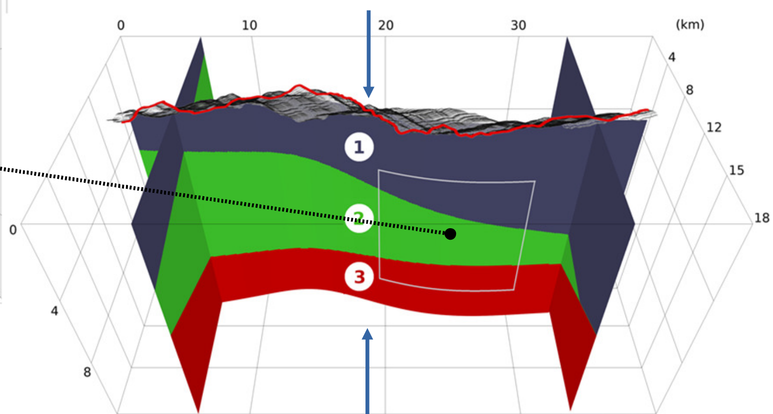

- *3 Layer - Modified "Widess" (1973) Model*

28

Synthetic Data Comparison (Straight)

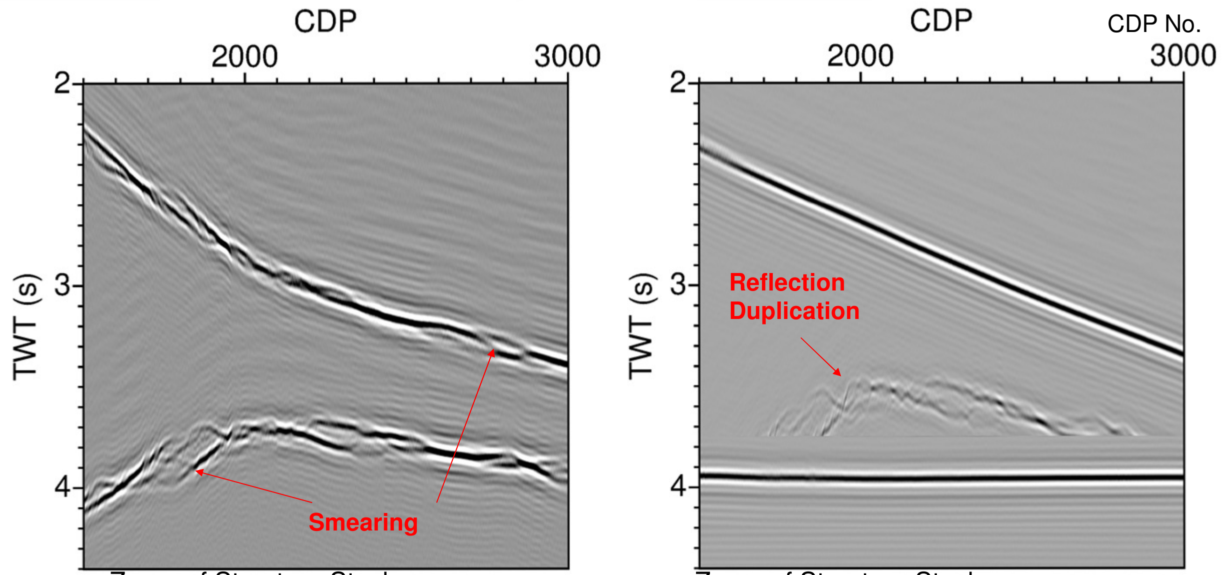

Zoom of Structure Stack (No CDMO)

Zoom of Structure Stack (With CDMO)

METAL EARTH 29

Synthetic Data Comparison (<u>Curved</u>)

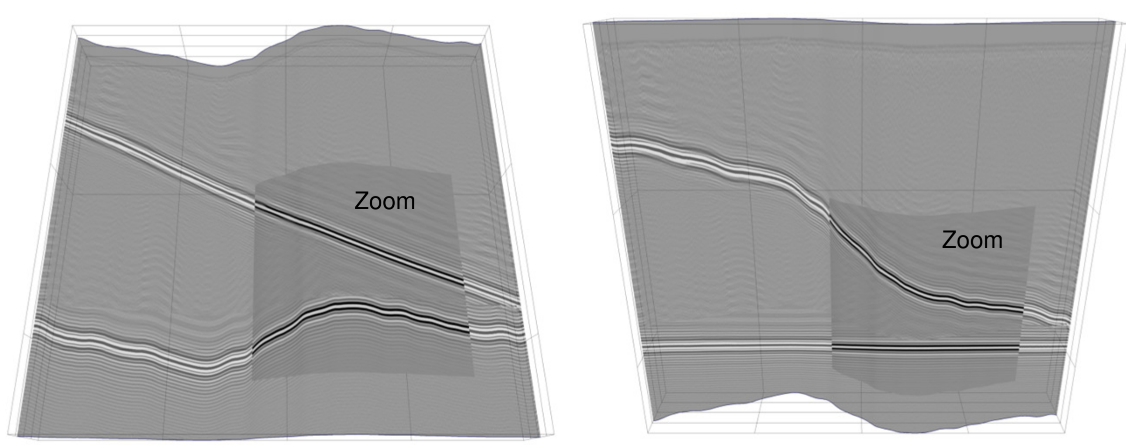

Perspective View of Structure Stack
Looking *Up* along plane of Top Reflection

Perspective View of Structure Stack
Looking *Down* along plane of Bottom Reflection

METAL EARTH 30

Synthetic Data Comparison

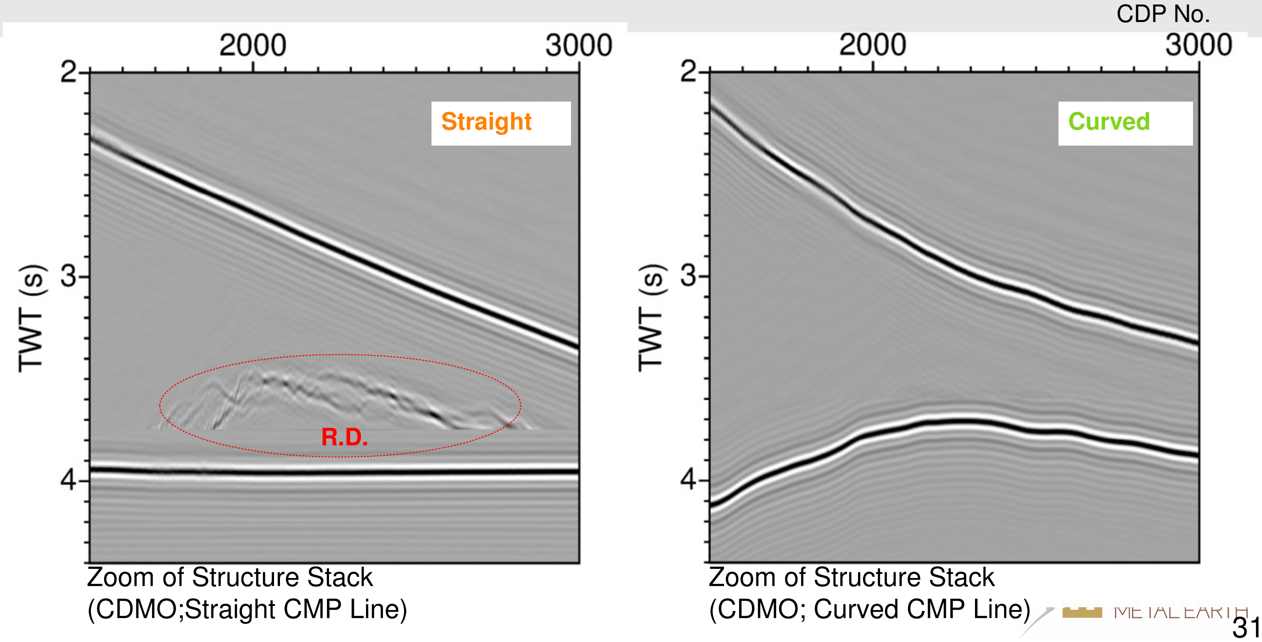

Field Data (Larder Lake)

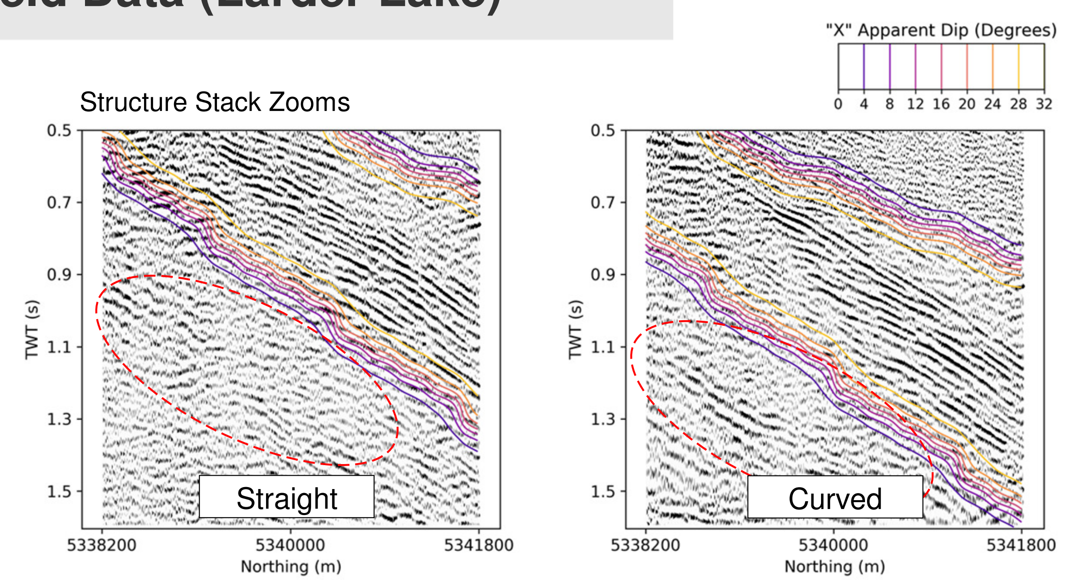

Curved binning CDMO processing results

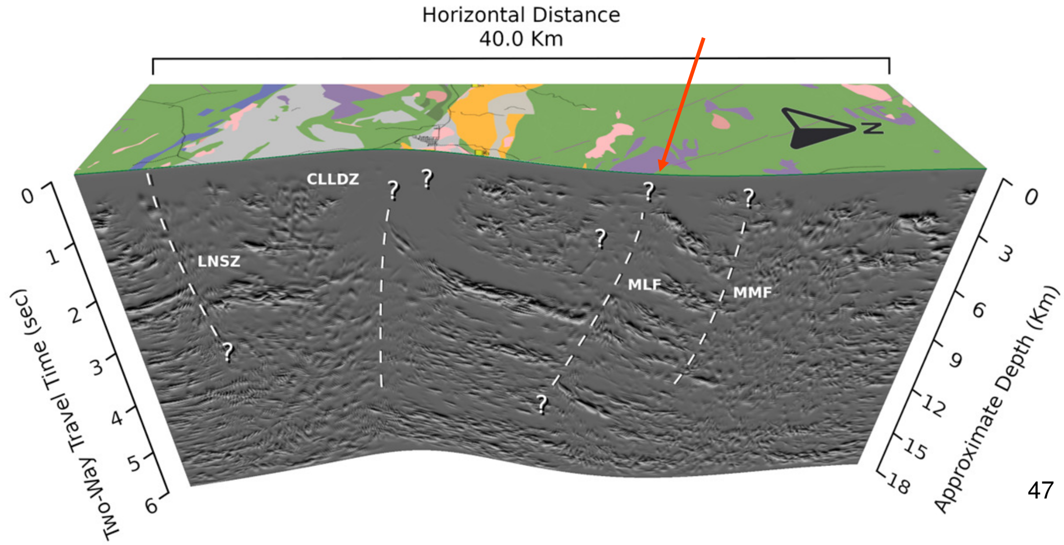

47

METAL EARTH

- Introduction
- Active Seismic Applications
  - Conventional Seismic Processing
  - Cross-Dip Move-Out (CDMO) corrections
  - Multi-focusing Imaging
  - Full Wave-Form (FWI) imaging
- Passive Seismic Application
  - Ambient Noise Surface Wave Tomography
  - Receiver Function analysis
- Integration and Interpretations
- Conclusions

METAL EARTH

Technical and theoretical challenges associated with crooked-line surveying

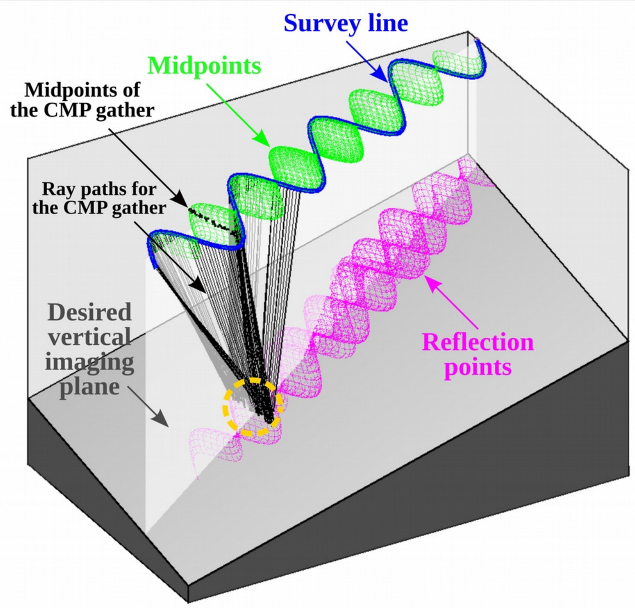

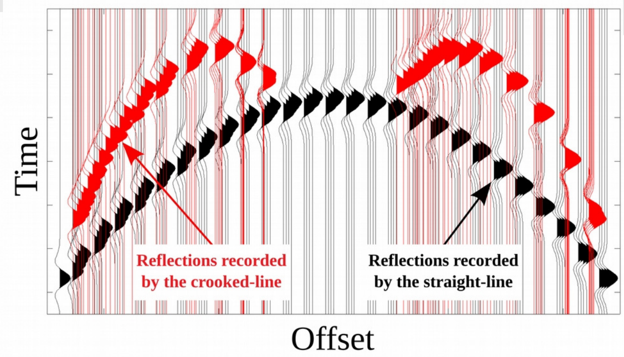

- Violates the assumption of a straight survey line
- Dispersion of the midpoints and reflection points
- Variable fold and uneven offset distribution
- Time and offset variant delay among reflections
- Defocusing and deformation of reflections (particularly from cross-dipped reflectors)

Multi-focusing (MF) basics

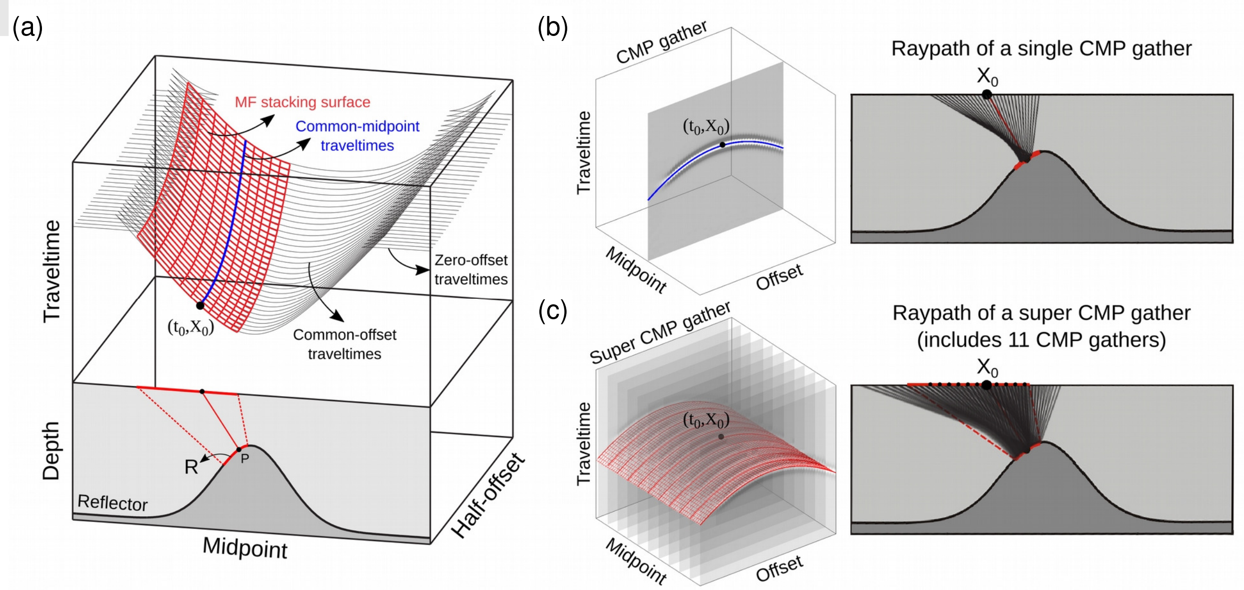

The basic principle of the multifocusing stacking method (adapted from Müller, 1999; modified after Abakumov, 2016)

Seismic processing steps

Prestack seismic data

Multi-focusing (MF)

- Building super CMP gathers
- Wavefield parameters analysis
- MF moveout correction
- Multifocusing stacking

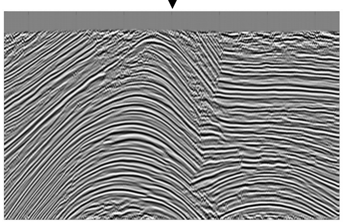

Conventional CMP stacking

- Building CMP gathers
- Stacking velocity analysis
- NMO Correction + DMO Correction + CDMO Correction
- Stacking

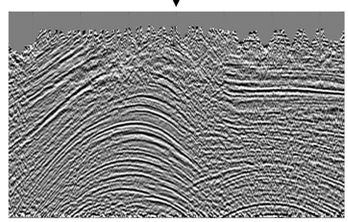

METAL EARTH

3D generalized spherical multi-focusing method

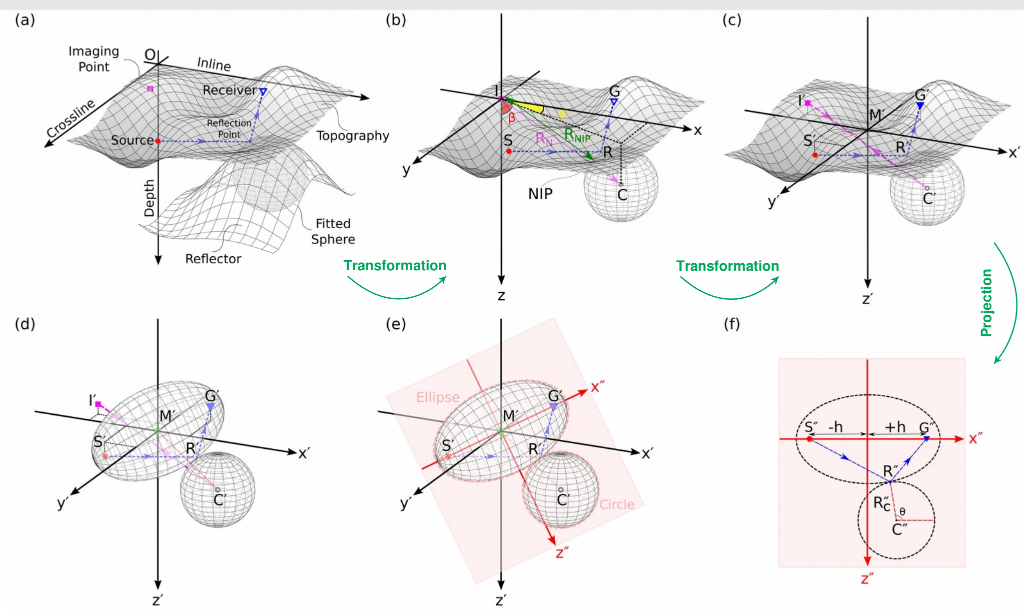

METAL EARTH

Larder Lake R2 High-resolution Seismic survey

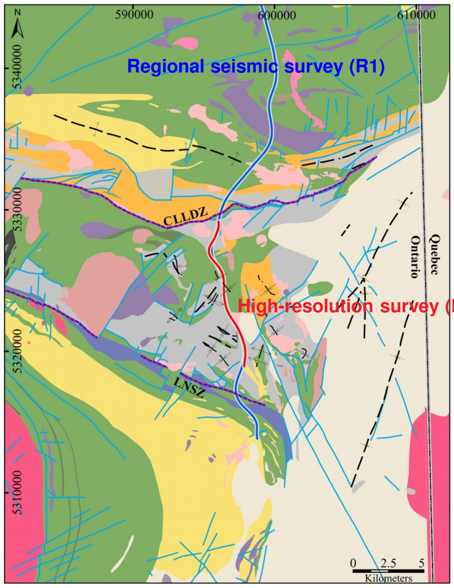

Acquisition Geometry	
Profile length	12.5 km
Receiver intervals	12.5 m
Number of shots	1494
Shot intervals	6.25 m

Geological map of the Larder Lake area.

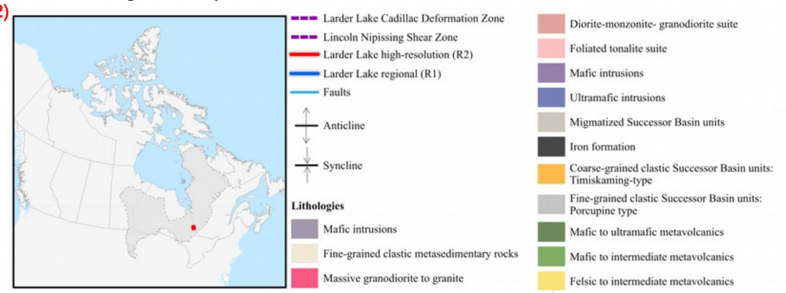

Signal processing and static corrections

A seismic Shot gather before **(a)** and after **(b)** signal processing and static corrections.

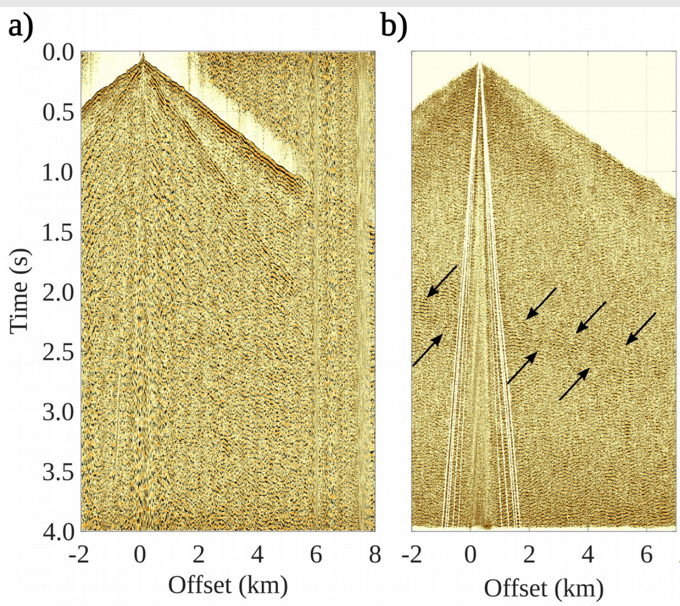

METAL EARTH

Wave-field Parameter Panels

V_0 = 5.5 km/s
$1/R_N$ = 0

The estimated 2.5D MF parameters and coherence function using a nonlinear global optimization algorithm.

a) The apparent dip along the north-south direction,
b) The apparent dip along the east-west direction,
c) The radius of normal-incident point wave curvature, and
d) The coherence section.

All sections are shown in colour superimposed on the 2.5D MF stack section.

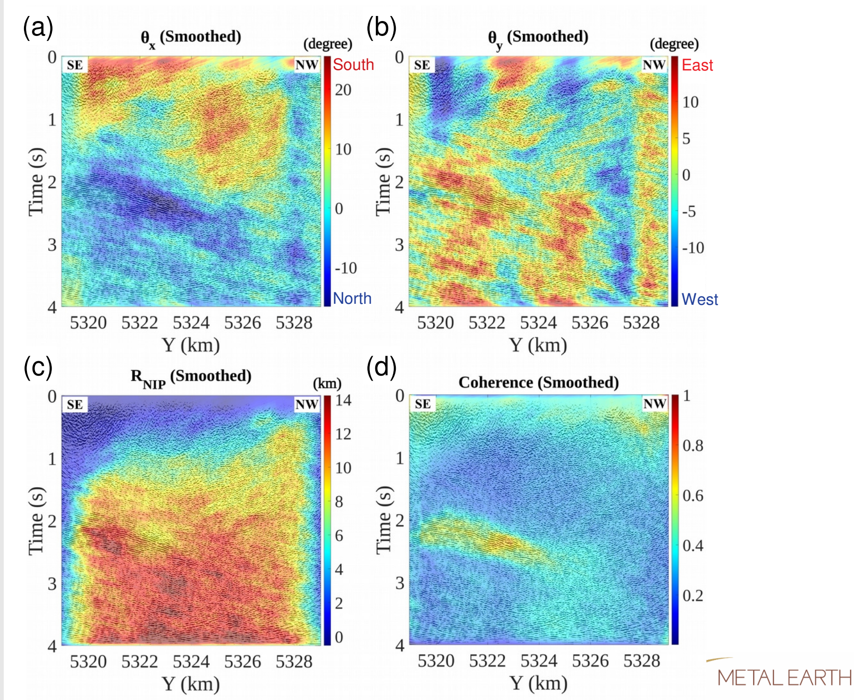

Stack sections

Comparing stack sections obtained by:

a) conventional (NMO stack),

b) conventional (NMO+DMO+CDMO stack),

c) 2.5D MF methods.

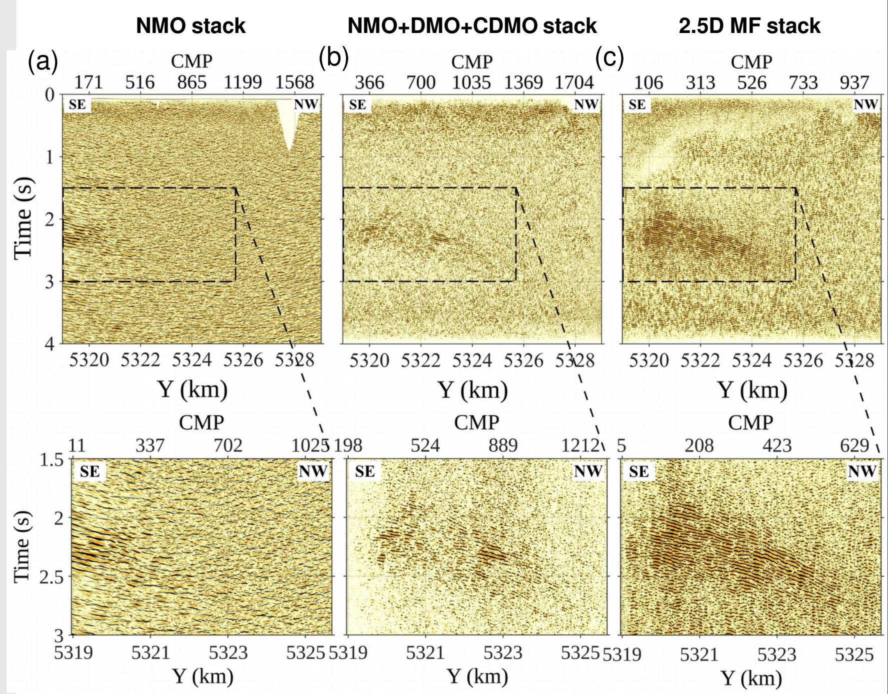

Migrated sections

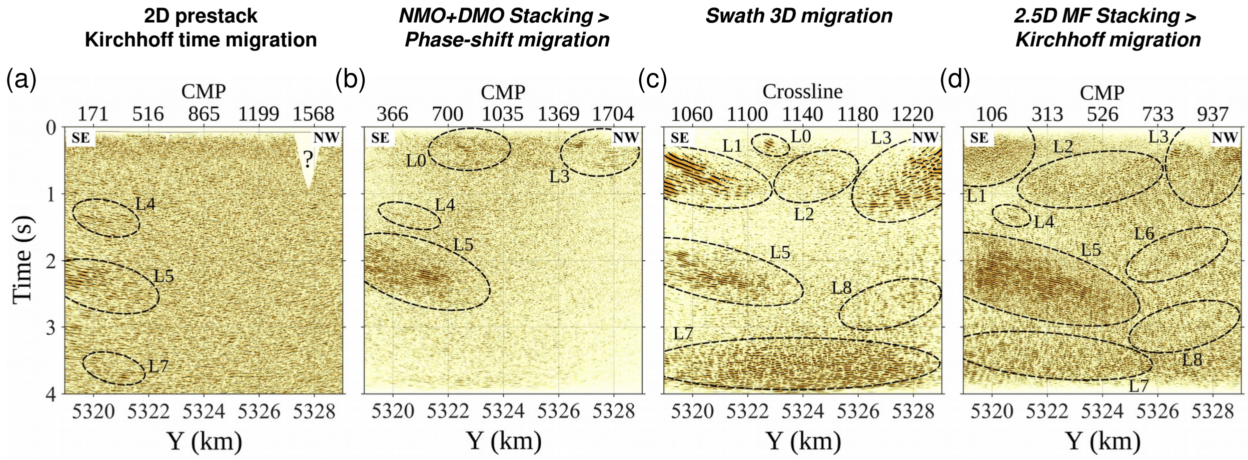

Migrated sections of the Larder Lake R2 seismic data set

METAL EARTH

- Introduction
- Active Seismic Applications
  - Conventional Seismic Processing
  - Cross-Dip Move-Out (CDMO) corrections
  - Multi-focusing Imaging
  - Full Wave-Form (FWI) imaging
- Passive Seismic Application
  - Ambient Noise Surface Wave Tomography
  - Receiver Function analysis
- Integration and Interpretations
- Conclusions

METAL EARTH

Full Wave-Form Inversion (FWI)

- Preprocessing
  - Numerical solution should represent observed data

Observed Data

Adapting Scientific Theory
- Acoustic and Isotropic Forward/Inverse Problem

Seismic Events Removal
- Elastic modes
- Surface waves
- Random noise

Geometry Management
- Coordinate projection
- Source-receiver offset preservation

Seismogram Treatment
- Low-pass frequency filters
- First breaks muting
- Removal of traces without traveltime picks
- Resampling in the time domain
- Filters in the frequency/wavenumber domain
- Amplitude correction – surface consistent
- Removal of traces with out-of-plane offsets

Monochromatic maps showing the real part of frequency-domain observed wave-fields at 7 Hz (left) before and (right) after data preconditioning. A more coherent and continuous pattern emerges after removing contaminating energy not modeled by the mathematical approximation (e.g., elastic modes, surface waves, etc.)

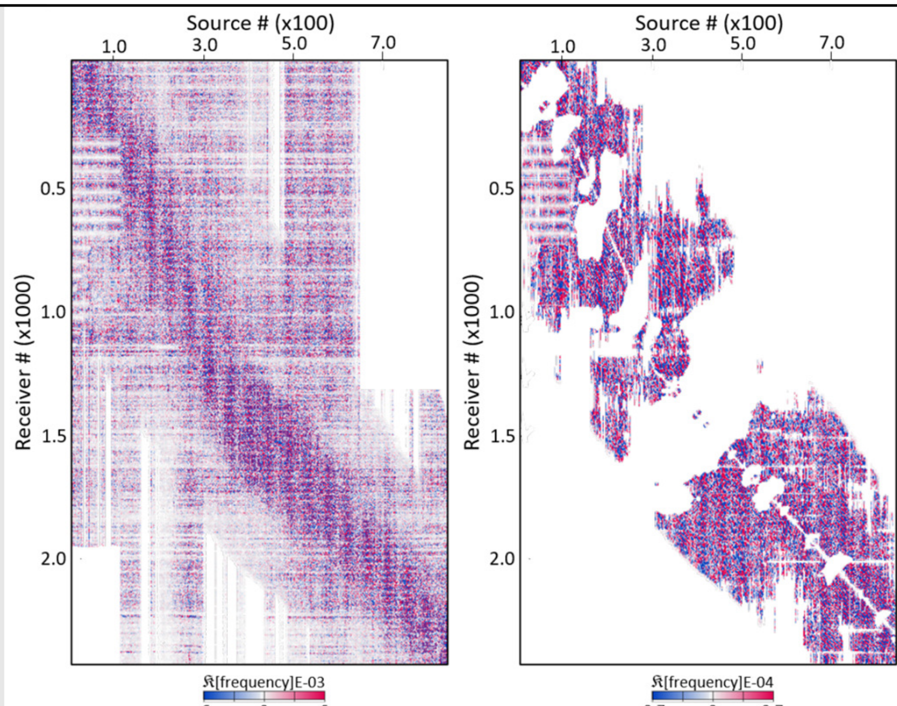

Full-waveform inversion ("FWI")

- 846 manually picked shot gathers
- Macro-velocity model
- 3D tomography – full geometry accounted for
- RMS misfit ~ 20 ms

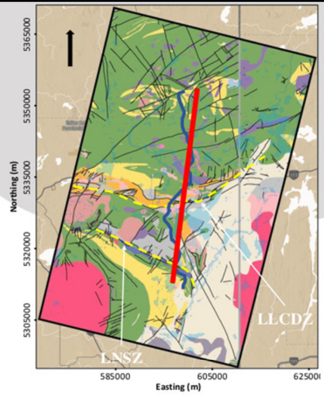

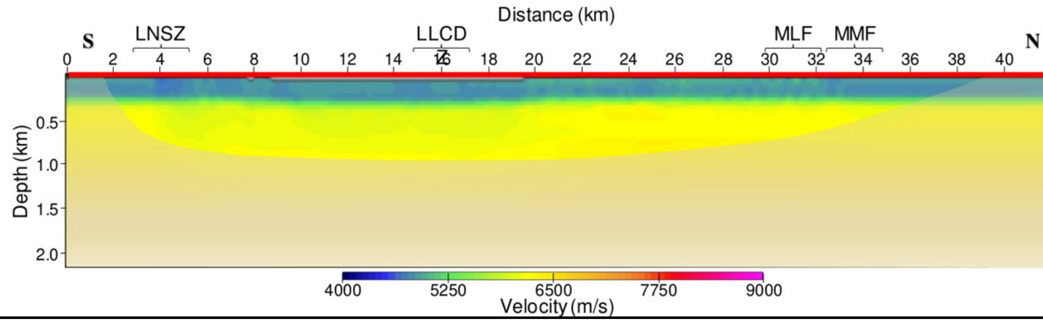

Full-waveform inversion ("FWI")

- 2D full-waveform inversion
  - Quantitative interpretation in terms of true velocity structures
  - Major structural domains are recovered in both 2D and 2.5D FWI models
  - Substantial differences in finer structural details – 2.5D improves imaging

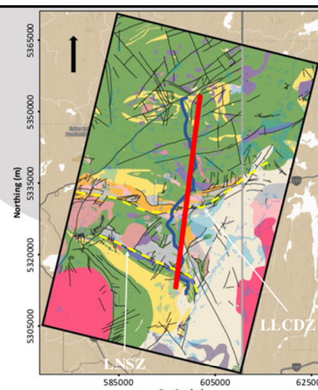

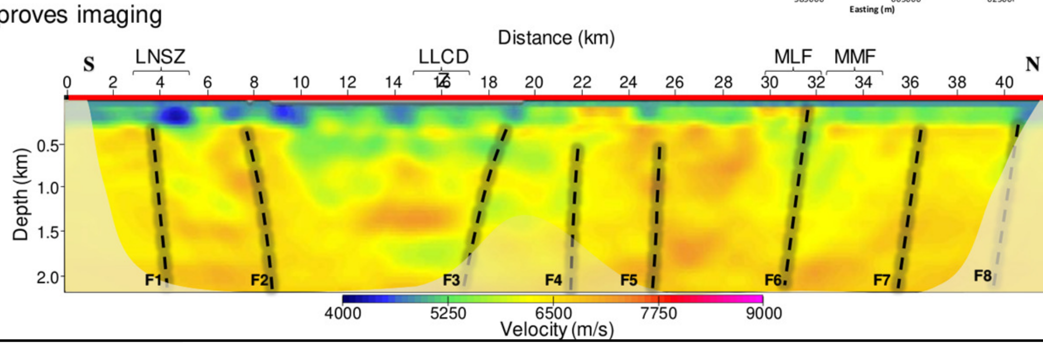

Full-waveform inversion ("FWI")

- 2.5D full-waveform inversion
  - Quantitative interpretation in terms of true velocity structures
  - Major structural domains are recovered in both 2D and 2.5D FWI models
  - Substantial differences in finer structural details – 2.5D improves imaging

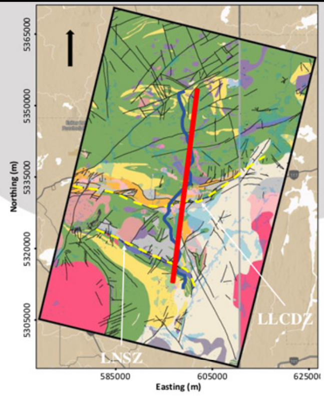

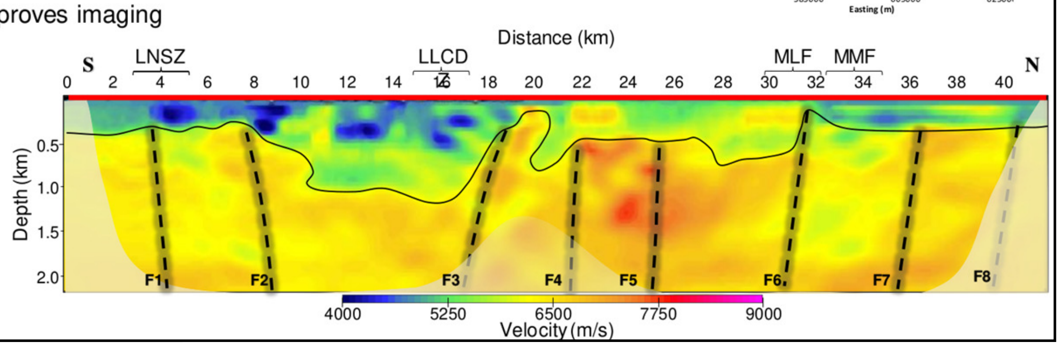

2D Vs. 2.5D Visco-Acoustic Full Wave-Form Inversion (FWI)

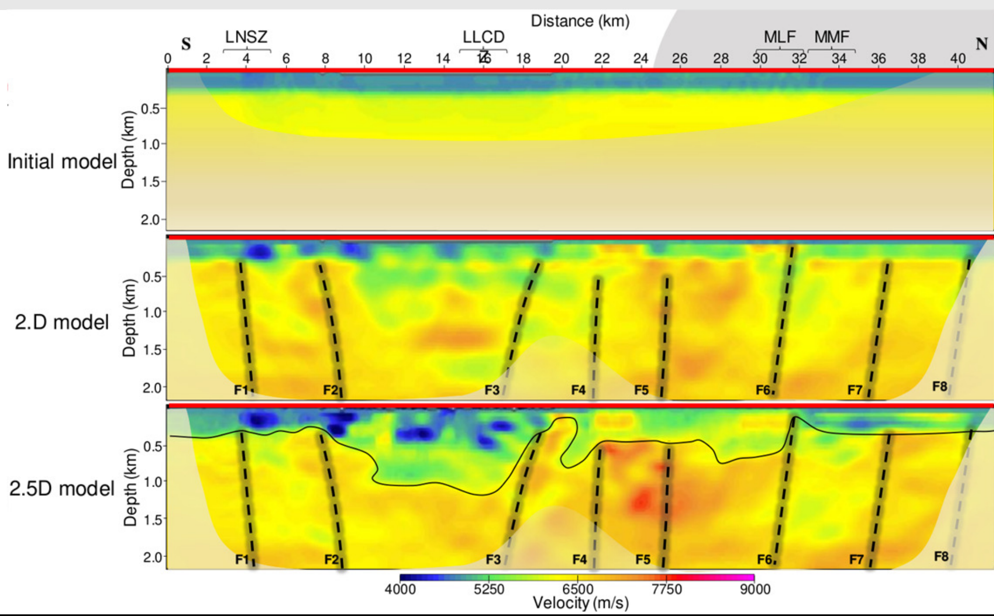

METAL EARTH

Outline

- Introduction
- Active Seismic Applications
  - Conventional Seismic Processing
  - Cross-Dip Move-Out (CDMO) corrections
  - Multi-focusing Imaging
  - Full Wave-Form (FWI) imaging
- Passive Seismic Application
  - Ambient Noise Surface Wave Tomography
  - Receiver Function analysis
- Integration and Interpretations
- Conclusions

METAL EARTH

Probabilistic power-spectral density (PPSD) plots of 4 passive seismic stations

The gray curves on the plots show the low and high limits for viable ambient noise signals. The PPSD plot of station LL10 shows signal outside the acceptable limit and therefore it was excluded for interstation group velocity estimations.

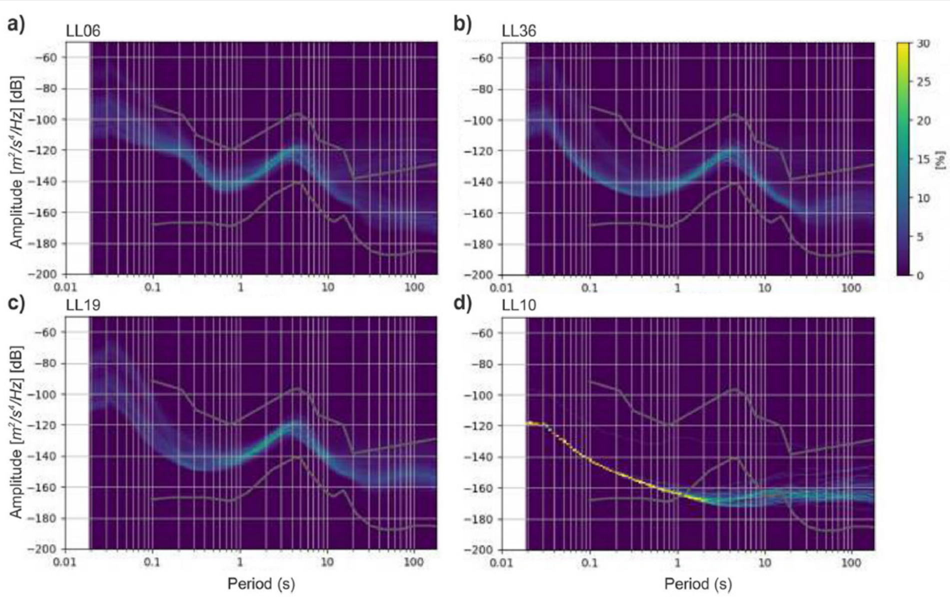

(a) and (b) show all of the horizontal-horizontal (TT) and vertical-vertical (ZZ) cross-correlations of ambient noise, respectively, sorted by increasing interstation distances. (c) Surface-wave dispersion curve estimated between the stations LL01 and LL23. (d) The estimated group velocity values for all possible pairs of stations with a minimum interstation distance of 10 km at 3-s period (notice that the longitude axis is stretched in this plot).

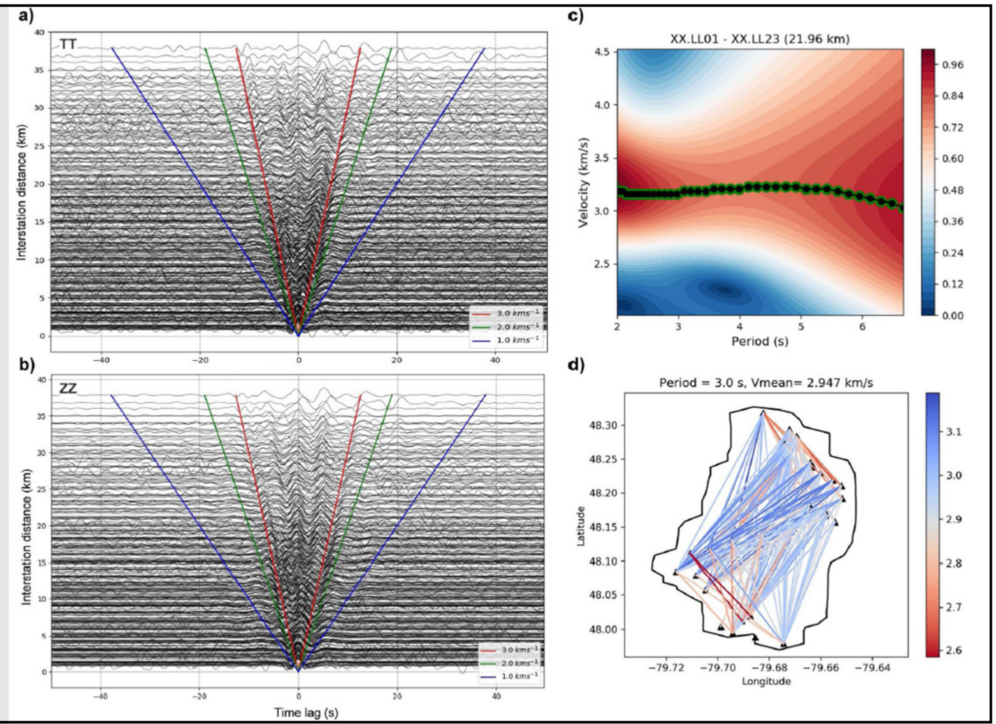

(a) Lithological map of the Larder Lake area in the vicinity of the passive seismic array. The curved black line shows the location of ME321-R1 seismic transect. The region marked by the black rectangle is the same as the dashed rectangle C in Figure 1a. (b) to (f) show the depth slices of the estimated shear-wave velocity using the ambient noise surface wave tomography (ANSWT) method at depths of 1, 3, 5, 7, and 9 km, respectively. The dimmed regions of the model have > ±50 m/s uncertainty for the estimated shear-wave

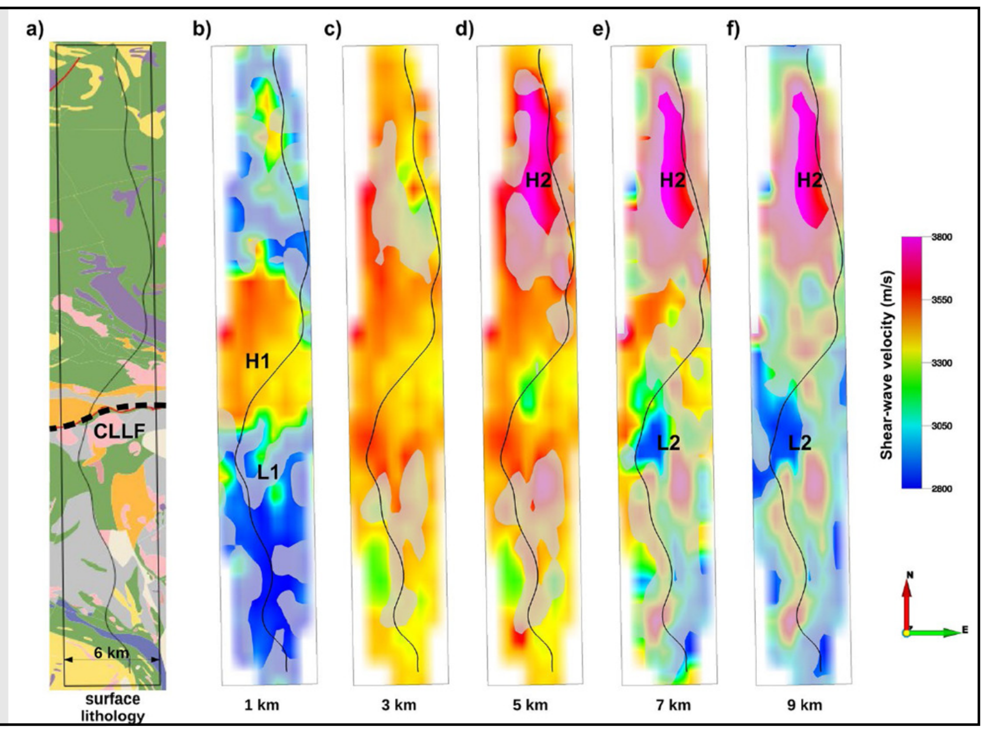

METAL EARTH

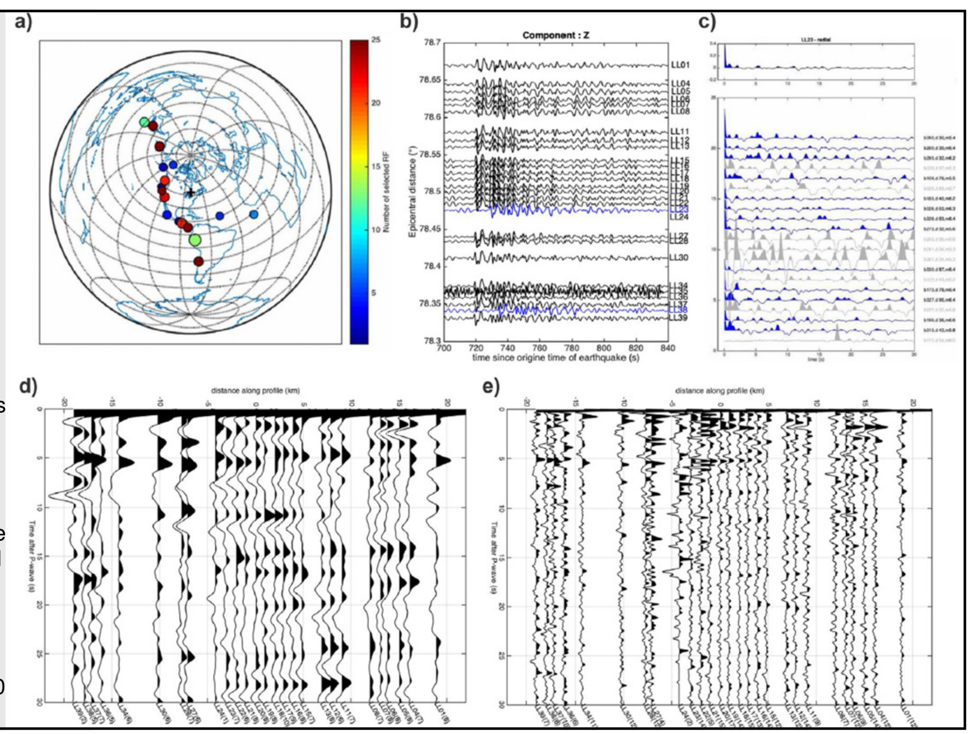

(a) The location of earthquakes used for receiver function (RF) analysis (the size of circles represents the magnitude of the earthquakes and the color represents the number of selected RFs). (b) The vertical component of a seismographs recorded by Larder Lake array from an earthquake in Chile. The blue traces were time-shifted due to timing issues and were corrected before further analyses. (c) The estimated RFs for the radial components of station LL23 from different earthquakes (bottom) and final stacked RFs (top). The gray-colored RFs were discarded due to the high level of noise. (d and e) The final estimated RFs for Larder Lake passive seismic stations for the very low frequency (VLF; 0.1–0.5 Hz) and high frequency (HF; 0.5–2.0 Hz) ranges, respectively.

(a)–(d) are the P-S convertibility profiles estimated using the receiver function (RF) analysis for the very low frequency (VLF; 0.1–0.5 Hz), low frequency (LF; 0.2–0.8 Hz), high frequency (HF; 0.5–2.0 Hz), and very high frequency (VHF; 0.8–3.0 Hz) bands, respectively. The convertibility is a similar concept to the reflectivity; however, it is an indication of elastic rock property variations in the subsurface that results in P to S wave conversions. The Moho discontinuity at depth of ~40 km and a south-dipping feature (S1) were imaged in all four frequency bands.

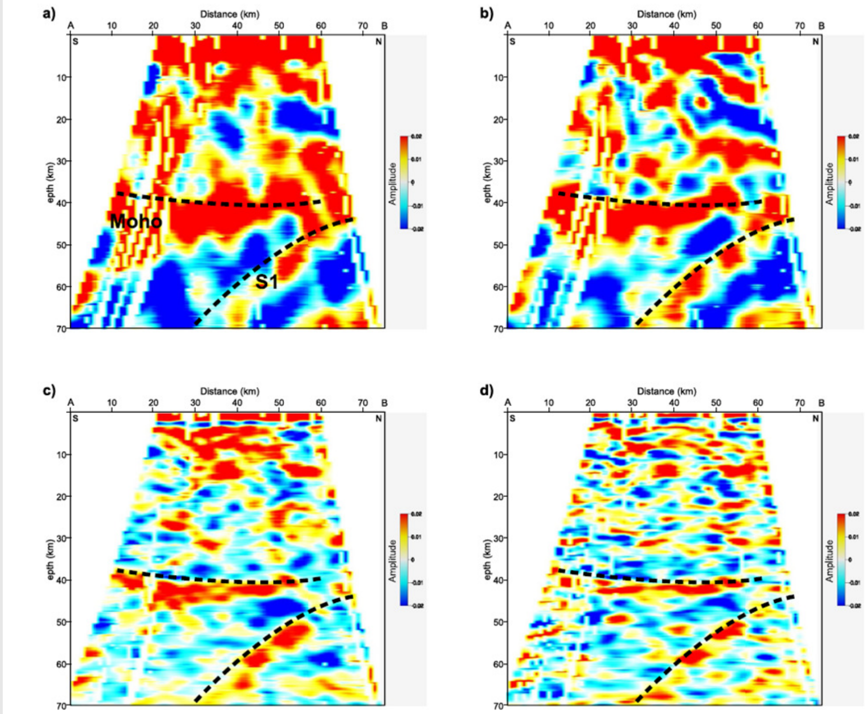

- Introduction
- Active Seismic Applications
  - Conventional Seismic Processing
  - Cross-Dip Move-Out (CDMO) corrections
  - Multi-focusing Imaging
  - Full Wave-Form (FWI) imaging
- Passive Seismic Application
  - Ambient Noise Surface Wave Tomography
  - Receiver Function analysis
- Integration and Interpretations
- Conclusions

METAL EARTH

(a) and (b) show the KSZ12 transect acquired as part of Lithoprobe project overlaid by lithological assemblages and magnetic maps, respectively. (c) and (d) show the Metal Earth's Larder Lake ME321 transect overlaid by the lithological assemblages and magnetic maps, respectively. The locations of Cadillac-Larder Lake Fault (CLLF) and Porcupine-Destor Fault (PDF) are shown on the lithological assemblage's map with dashed lines. The white circles in (d) highlight the magnetic responses of syn-tectonic felsic intrusions.

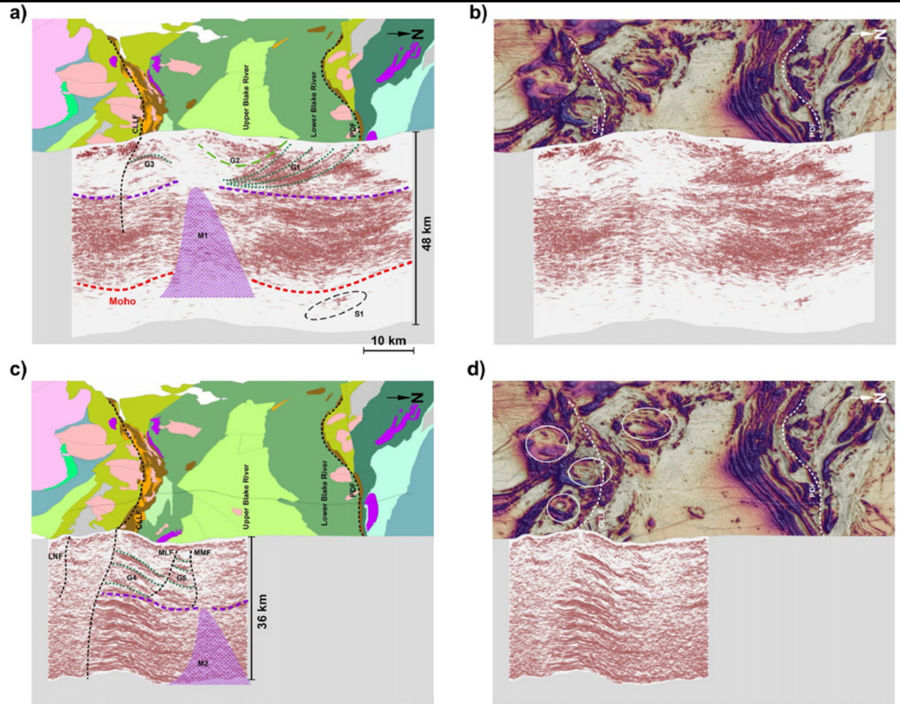

(a) The projection of the estimated shear-wave velocity using ambient noise surface wave tomography (ANSWT) method on the ME321-R1 seismic transect. (b) The projection of the shear-wave velocity estimated using ANSWT method on the ME321-R1 seismic transect where parts of the model with an uncertainty of ±50 m/s for the estimated shear-wave velocity were dimmed using a semitransparent gray tone. The shear-wave anomalies L1, L2, H1, and H2 have a high certainty making them more reliable for geological interpretation purposes.

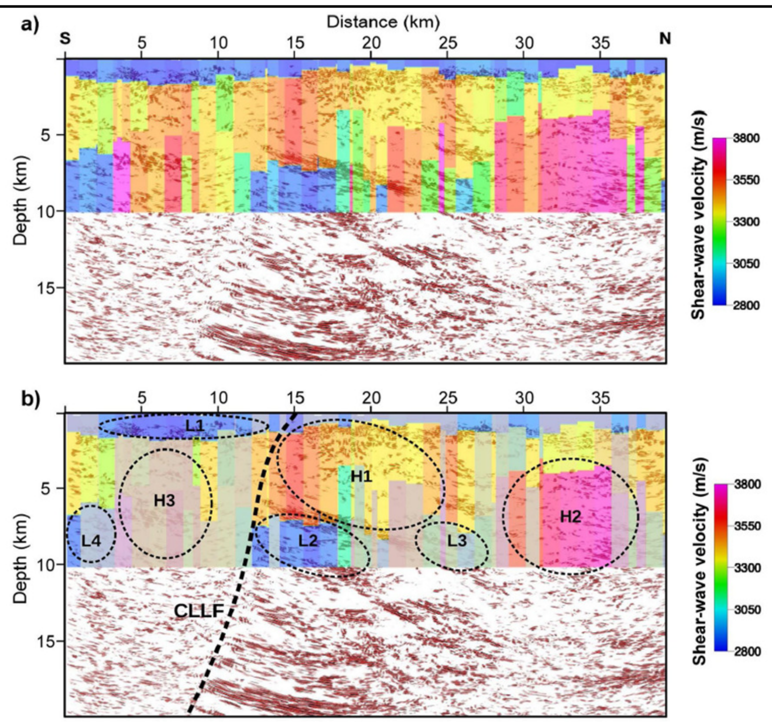

The P-S convertibility profile (the average of all frequency bands) estimated using the receiver function (RF) method overlaid on the ME321-R1 seismic transect. The shallow C1 and C2 anomalies have good correlation with the active seismic and ambient noise surface wave tomography (ANSWT) model. The C3 anomaly reside on the bottom of the upper crust indicating a significant elastic property change from upper crust to lower crust. The C4 anomaly overlies a zone of strong reflections to the north of the Cadillac-Larder Lake Fault (CLLF).

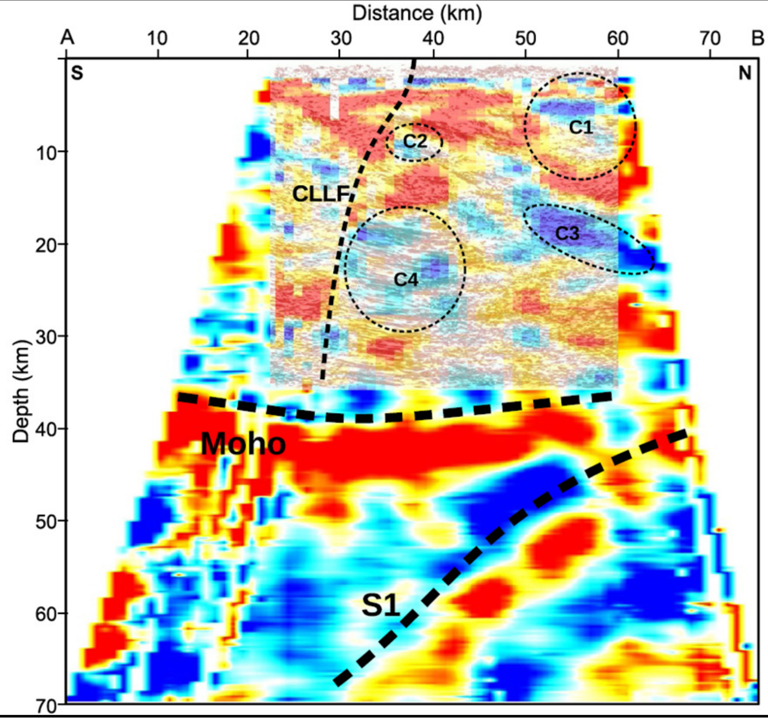

The top 10 km of the (a) reflection seismic, (b) ambient noise surface wave tomography (ANSWT) shear-wave velocity, and (c) P-S convertibility transects. The B1, B2, and B3 features are highly correlated between all three transects. The P1, P2, and P3 features also show noticeable correlation though with low certainty.

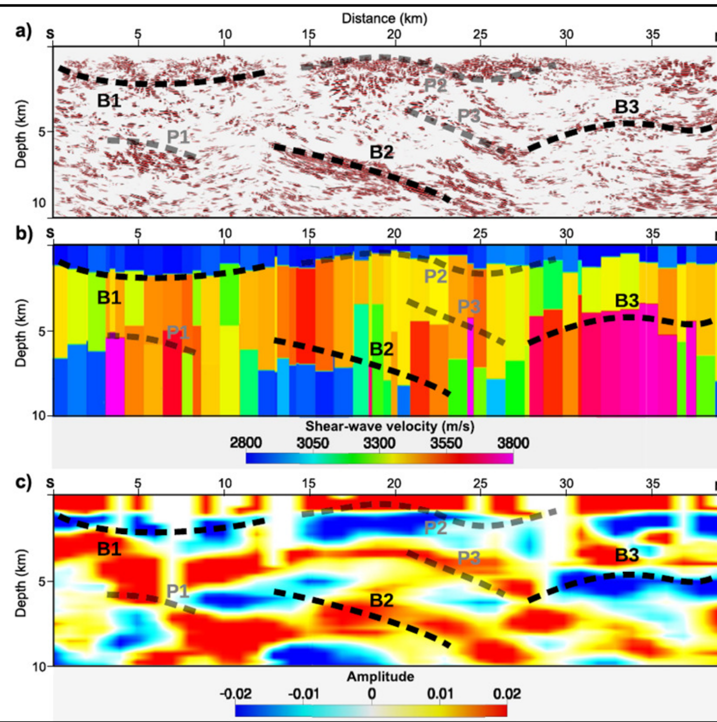

Integrated interpretation of the ME321-R1 and KSZ12 seismic lines and the deeper part of the P-S convertibility transect derived from receiver function (RF) analysis. The G2 marks the depth of upper Blake-River volcanic units. The R1 and R2 show the base of the greenstones beneath the KSZ12 and ME321-R1 transects, respectively. The greenstones are 2–3-km thicker under the ME321-R1 transect. The S1 feature shows as package of strong reflection below the Moho on the KSZ12 transect and extends to the depth of 70 km (the depth limit of the RF analysis). The R3 and R4 mark the bottom of middle-crust and lower-crust regions. The dimmed reflectivity zone, M2, beneath the ME321-R1 similar to the M1 zone beneath the KSZ12 is likely caused by intrusions from the mantle due to the

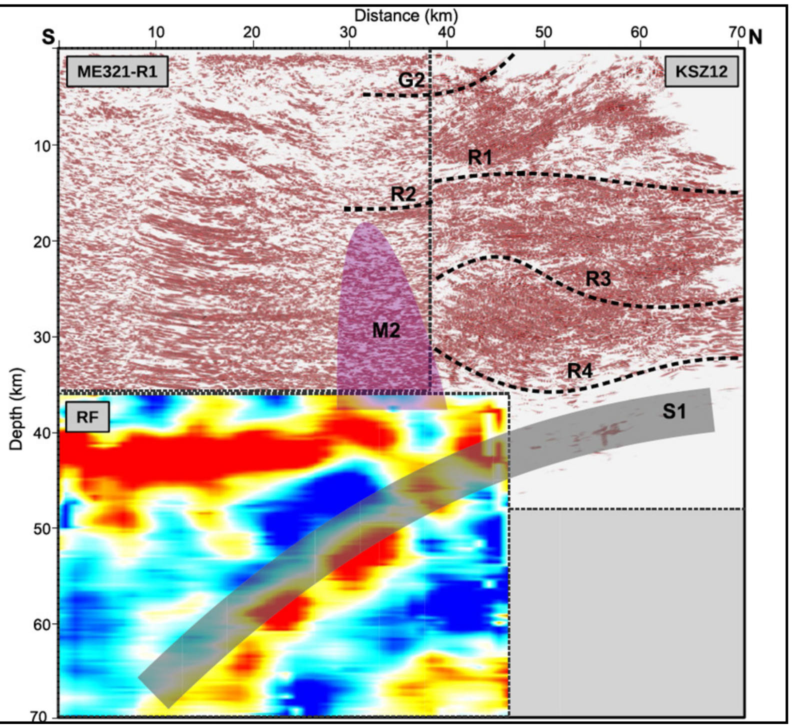

Conclusions I

- Metal Earth has acquired **16 R1 (regional)** and **13 R2 (high-resolution)** seismic surveys.
- More than **60 Lithopobe seismic transects** were downloaded and their coordinates were remapped and cleaned up, making them suitable to be viewed in **3D geological visualization** software.
- **Seismic data processing** plays a crucial role in obtaining high-resolution and reliable subsurface images from active (reflection) seismic surveys. We have developed/applied state of art processing methods such as **Cross-Dip Move-Out (CDMO), Multi-Focusing (MF), and Full Waveform Inversion (FWI)** to effectively and accurately image seismic reflection from crooked-line 2D Seismic surveys.
- We have acquired **co-located active and passive seismic surveys** over a metal-endowed Archean granite-greenstone terrane in the Larder Lake area to investigate the reliability of estimated elastic properties using passive seismic methods.

METAL EARTH

Conclusions II

- The passive seismic data were processed using two different data processing approaches, **ambient noise surface-wave tomography (ANSWT)** and **receiver function analysis**, to generate **shear-wave velocity** and **P to S wave (P-S) convertibility** profiles of the subsurface, respectively.
- The **Cadillac-Larder Lake Fault (CLLF)** was imaged as a **south-dipping sub-vertical zone of weak reflectivity** in the reflection seismic profile.
- A package of north-dipping reflections in the upper crust (at depths of 5–10 km), to the north of the CLLF, resides on the boundary of high (on the top) and low (on the bottom) shear-wave velocity zones estimated using the ANSWT method. This package of reflections is most likely caused by **overlaying mafic volcanic and underlying felsic intrusive rocks**.
- The **P-S convertibility profile** imaged the **Moho boundary at ~40-km** depth as well as a **south-dipping feature that penetrates the mantle**, which is interpreted to be either caused by the **delamination of the lower crust** or a possible **deeper extension of the Porcupine-Destor Fault**.

METAL EARTH

Acknowledgments

- Dr. Hossein Jodeiri Akbari Fam, Christopher Mancuso, Dr. Brian Villamizar, and
- SAExploration Ltd., Seismic Data Acquisition
- Absolute Imaging Inc., Seismic Data Processing
- Metal Earth and MERC Staff (Administration, Faculty, PDFs, Students, …)
- Harquail School of Earth Sciences
- OpendTect, QGIS, Seismic Unix, Octave, Curve-Labs software developers.

METAL EARTH

References

Mints, M. V., 2017; The composite North American Craton, Superior Province: Deep crustal structure and mantle-plume model of Neoarchaean evolution; Precambrian Research, 302, pp. 94–121.

Montsion, R., Thurston, P., Ayer, J., 2018, 1:2 000 000 Scale Geological Compilation of the Superior Craton – Version 1: Mineral Exploration Research Centre, Harquail School of Earth Sciences

Naghizadeh, M., Snyder, D., Cheraghi, S., Foster, S., Cilensek, S., Floreani, E., and Mackie, J., 2019; Acquisition and Processing of Wider Bandwidth Seismic Data in Crystalline Crust: Progress with the Metal Earth Project, Minerals, 9(3), 145.

Percival, J. A. 2007; Geology and metallogeny of the Superior Province, Canada; In Mineral Resources of Canada: A Synthesis of Major Deposit Types, District Metallogeny, the Evolution of Geological Provinces, and Exploration Methods. Edited by W.D. Goodfellow. Geological Association of Canada, Mineral Deposits Division, Special Publication No. 5, pp. 903–928.

Perron, G. and Calvert, C. J., 1998; Shallow, high-resolution seismic imaging at the Ansil mining camp in the Abitibi greenstone belt, Geophysics, 63, no. 2, 379-391.

Zipped SEGY files of Lithoprobe Transects: http://ftp.geogratis.gc.ca/pub/nrcan_rncan/vector/lithoprobe/zipped_segys/; Released to public under Open Government Licence – Canada : https://open.canada.ca/en/open-government-licence-canada

METAL EARTH